Second Quarterly Report | *Covering the Period 1 October to 31 December 1965*

9 February 1966

STUDY AND APPLICATIONS OF RETRODIRECTIVE AND SELF-ADAPTIVE ELECTROMAGNETIC WAVE CONTROLS TO A MARS PROBE

Prepared for:

NATIONAL AERONAUTICS AND SPACE ADMINISTRATION
TECHNICAL INFORMATION DIVISION
AMES RESEARCH CENTER
MOFFETT FIELD, CALIFORNIA

CONTRACT NAS 2-2933

By: C. A. HACKING C. H. DAWSON R. C. KUNZELMAN J. A. MARTIN L. A. ROBINSON

SRI Project 5574

Approved: R. C. HONEY, MANAGER
ELECTROMAGNETIC TECHNIQUES LABORATORY

D. R. SCHEUCH, EXECUTIVE DIRECTOR
ELECTRONICS AND RADIO SCIENCES

Copy No. 6

ABSTRACT

Computer studies have been continued of three different cylindrical antenna configurations that could be used as adaptive arrays for deep space vehicles. Analysis of the effects of vehicle spin on gain modulation has been made. Some effects of spin on spectral splitting are superficially discussed but have not yet been analyzed.

The effects of planetary reflections on a retrodirective array system have been studied.

Some system aspects of a planetary mission employing retrodirective arrays are considered. A start has also been made on studying the use of an adaptive array to provide navigational information such as angle of arrival of a signal.

CONTENTS

ILLUSTRATIONS

TABLES

I INTRODUCTION

This is the second quarterly progress report of a study to investigate some of the many possible uses of adaptive antenna circuits for communication, to and between vehicles on an interplanetary mission. It is assumed that the main vehicle, the bus, flies by or orbits the target planet and when in the vicinity releases a smaller vehicle, the capsule, to enter the planet's environment for a hard or soft landing. Communication between the earth and the bus is specified as being within the presently used *S*-band of frequencies, but between the bus and capsule the best frequency of operation is yet to be established. In addition to communication, the adaptive antenna circuitry should be considered for other purposes as well, such as providing navigational and environmental information.

In the first quarterly progress report the analysis was started of a particular cylindrical antenna configuration in which all the receiver/transmitter elements are used for any azimuthal direction of the antenna beam. This was done by focusing the energy to and from the elemental radiators by means of a cylindrical geodesic lens. For this antenna the computed gain was generally less than one dB below the postulated theoretical maximum value and required no switching of elements as the vehicle rotated.

The first Quarterly Progress Report also included a study of the conditions to be expected in the vicinity of Mars, particularly as they would relate to communications with a capsule entering the Martian environment.

During this second quarter, work has progressed on all three of the tasks, which are re-enumerated below. Each task is under a task leader, but it has not been possible to keep the tasks isolated from each other as had been planned at the start of the project.

Task I-Antenna Concepts: System and analysis aspects of antenna configurations

Task II-Environmental Conditions: Specific environmental conditions and their effect on system and component configurations

Task III-Phase Lock Loops and Adaptive Circuitry: Circuitry behind the antenna elements.

A particularly important problem, which cannot conveniently be assigned exclusively to any one of the above tasks, is that of space vehicle spin. It is not discussed much in this report but will receive increasingly more attention in subsequent work. System study is another area which is difficult to categorize under the above task headings.

During the quarter, three additional particular antenna configurations were analyzed, while environmental effects and direction-finding techniques were studied without relating them to any particular configuration. Each configuration was treated as a retrodirective antenna, rather than as the more general self-adaptive antenna.

A start has also been made on the analysis of various communications systems which might be used on the proposed mission as well as the use of adaptive circuitry for obtaining directional information.

This second quarterly report incorporates the report for the sixth month of the contract.

At the end of the second quarter, 59 percent of the contract funds remained on the project. The average rate of expenditure of contract funds during the last month of the quarter has been equal to the average rate required for the contract as a whole. The rate of effort will therefore be increased slightly for the remaining two quarters of the contract.

II PERFORMANCE DURING THE SECOND QUARTER

A. TASK I—ANTENNA CONCEPTS

1. Basic Antenna Configurations of the Cylindrical-Lens Type

The first quarterly report[1*] included a fairly comprehensive analysis of the cylindrical-geodesic-lens biconical-horn adaptive antenna used as a retrodirective antenna. The mathematical techniques used for the analyses of this antenna were described and some of the computed antenna patterns were reproduced. A table of results showing comparative antenna gains derived in five different manners was also reproduced for eight antennas of the same general configuration but with different parameters. It was pointed out that the result of primary concern of a retrodirective antenna is the maximum effective radiated power (ERP) in the retrodirection. In the final analyses, it is therefore probably not necessary to compute the re-radiation pattern except as one method of obtaining an absolute value of the gain in the retrodirection. However, for the sake of completeness and because it was relatively easy and inexpensive to do so, most of the patterns for each of the variations of the first antenna configuration were computed.

a. DISCRETE-LINE-SOURCE RADIATOR CONFIGURATION

Mention was made in the first quarterly report that work had also started on a second basic antenna configuration, known as the discrete-radiator cylindrical-geodesic-lens antenna. This is shown in simplistic form in Fig. 1. During the second quarter, the computer analysis of this configuration was continued and some results obtained. As will be apparent from the theory of the analysis procedure, the computation necessary to obtain a single point of a retrodirective pattern is quite extensive and increases approximately as the square of the linear dimension of the antenna. Some effort was expended in trying to reduce the cost of computing each

* References are listed at the end of the report.

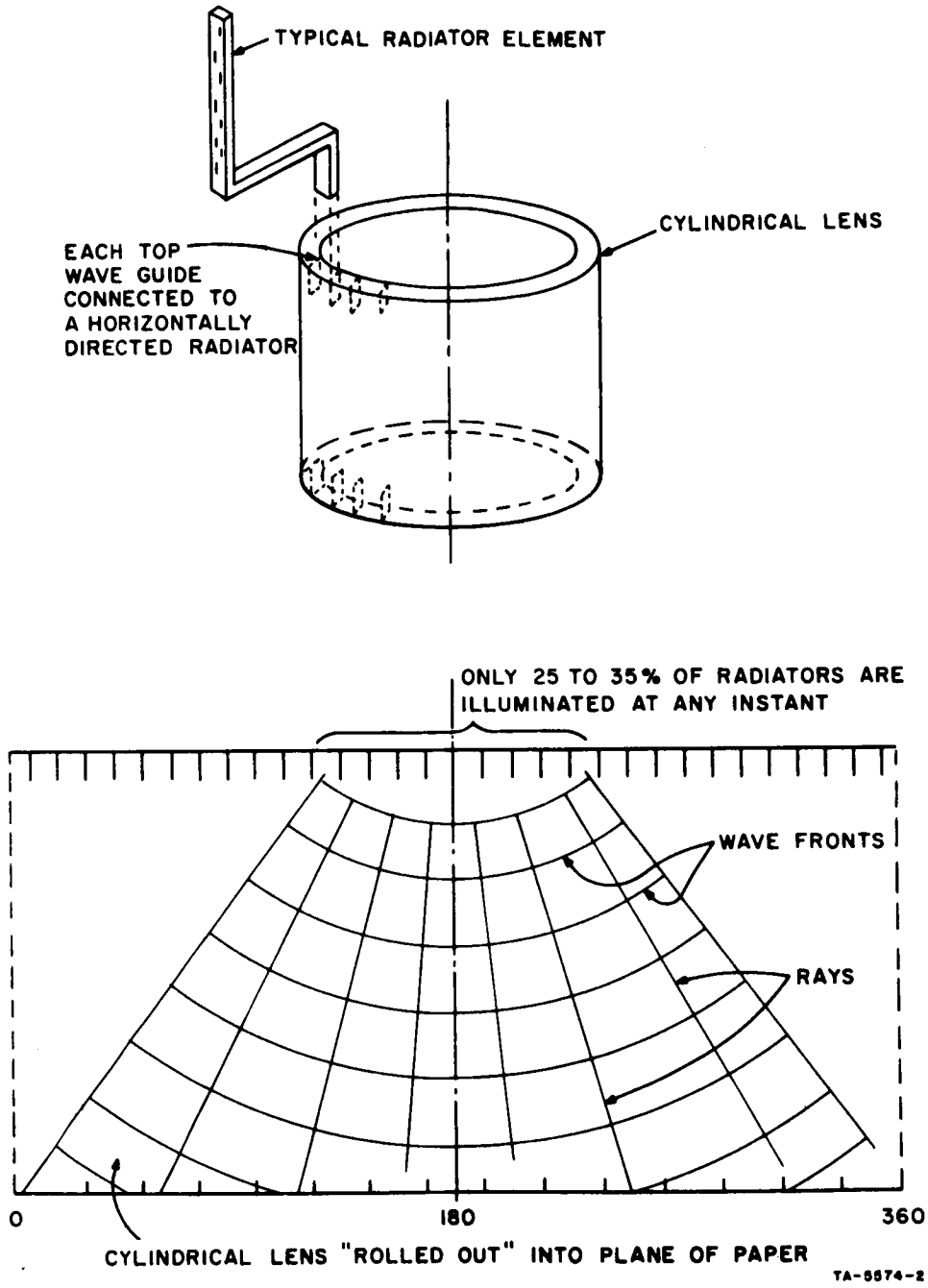

FIG. 1 A CYLINDRICAL-GEODESIC-LENS MULTIPLE-LINE-SOURCE ANTENNA

point by streamlining the computation procedure; however, it soon became obvious that the cost of computing complete retrodirective antenna patterns for each set of antenna parameters would be prohibitive. Since the shape of the main beam is an important characteristic of any antenna, a portion of the antenna pattern in the vicinity of the main beam was computed in a few cases. In other cases only the gain in the retrodirection was computed. Some effects of the variation in signal frequency, the effect of using a different frequency for receiving and transmitting from the same antenna, and the effects of rotation of the retrodirective antenna (vehicle spin) were investigated. Investigations of the extremely important effects of vehicle spin on signal spectrum will not, however, be reported in this present work.

b. THEORY OF ANALYSIS PROCEDURE

The basic cylindrical geodesic-lens multiple-line-source antenna is shown in Fig. 1. It consists of M elemental radiators each connected directly to a receiver/amplifier/transmitter, at what will be referred to as the bottom of the cylindrical geodesic lens. At the top of this lens are N waveguides, each feeding an identical line source radiator which has considerable gain in the axial or vertical direction but only 4 or 5 dB in the azimuthal direction. The peak of this radiation from each line source is assumed to be radially outward There are, of course, also N of these line source radiators.

Each of the M elemental radiators is coupled to each of the N line source radiators by several different coupling paths within the cylindrical geodesic lens. This is shown in Fig. 2 where the cylindrical lens is "rolled out" or developed into a flat plane so that the coupling can then be represented by straight lines between each of the two points considered to be coupled. There are an infinite number of coupling paths between any point at the bottom of the cylindrical lens to any point at the top but only three such rays will be assumed to exist in this analysis as shown in Fig. 2. The contributions from higher order ray numbers is in fact very small and will be assumed negligible. It can now be seen that in order to compute a single point in the far field radiation pattern of such a retrodirective antenna, it is necessary to sum the electric vectors from $N/2$ line source radiators. Each radiator is in turn coupled to M transmitters by three different paths. Another way of putting this is to say that each of the M amplifier/transmitters feeds each of the $N/2$ effective radiators by three different paths; thus, there are in effect $3N/2$ rays

contributing to each point in the radiation pattern from each elemental amplifier/transmitter. This compares with two rays for the biconical-horn antenna configuration previously reported.[1] Since the contribution from each ray must be added vectorially in the far field, the magnitude of computation becomes apparent.

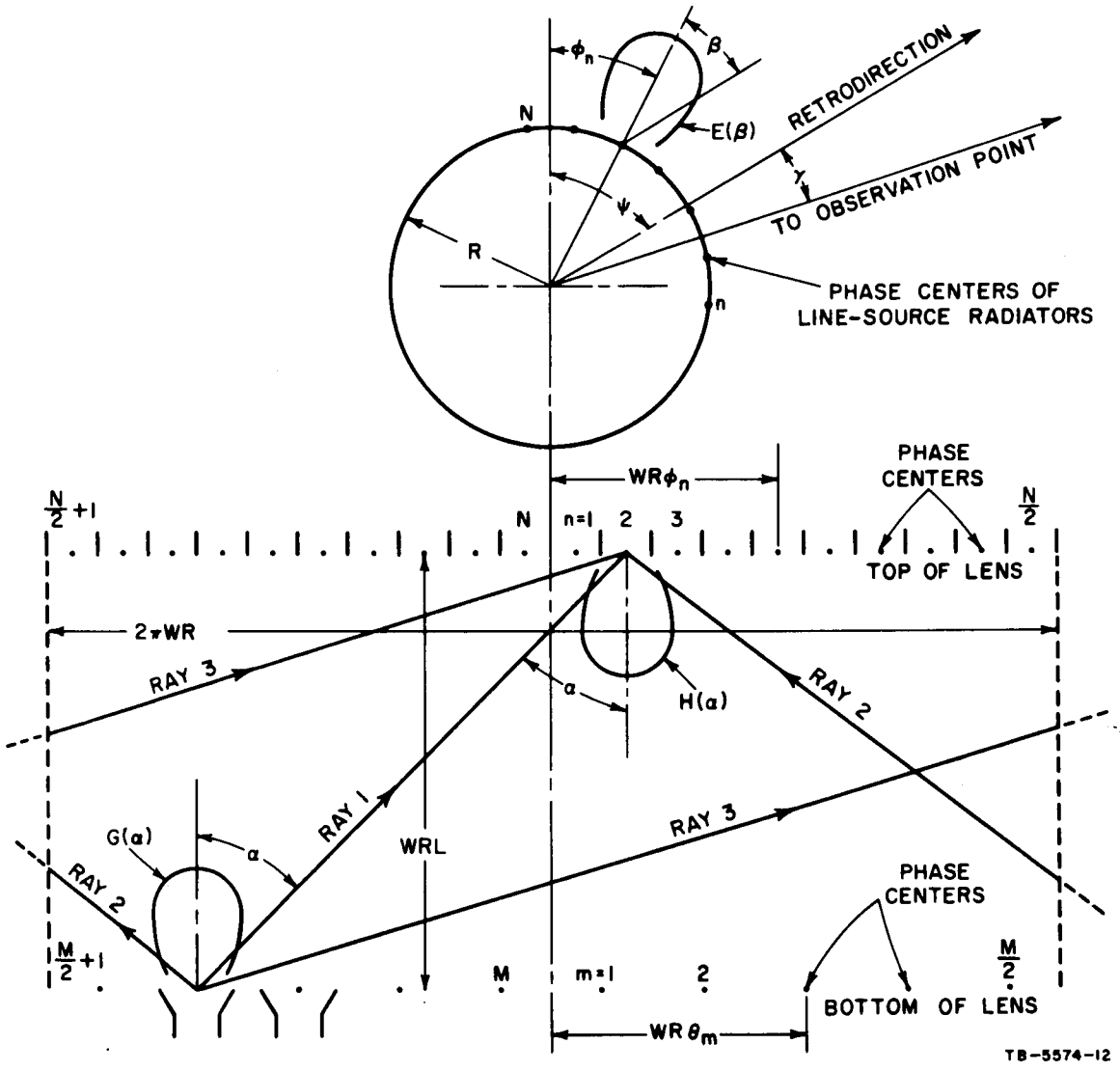

FIG. 2 GEOMETRY ASSOCIATED WITH A SINGLE GEODESIC-LENS RADIATOR AND A SINGLE LINE-SOURCE RADIATOR

c. COUPLING WITHIN THE GEODESIC LENS

As is demonstrated in Fig. 2, the coupling between any one of the M amplifier/transmitters and any one of the N waveguides at the top of the lens is the vector sum of three rays, the electric intensity of each being a function of the elemental radiation patterns of the two apertures at the ends of the lens, and the space attenuation between the two phase centers. It is, of course, quite conceivable that at some frequency the resultant vector could be zero, indicating no coupling between these two apertures.* Since the lens is a two-dimensional device, the space attenuation of power within the lens is assumed to be simply proportional to the inverse of ray length $WRL\lambda/\text{Cos}\ \alpha$, giving $\sqrt{\text{Cos}\ \alpha}$ as the amplitude space attenuation factor.

Other parameters of the antenna are defined below:

α_{mni} is the angle between the peak of the mth elemental radiator within the geodesic lens and the nth waveguide at the top of the lens, via the ith ray. In a right-cylindrical lens (see Fig. 2), the same angle applies between the ray and the peak of the elemental pattern of waveguide at the top of the lens. $(-\pi < \alpha < \pi)$.

$\beta_{n\gamma}$ is the angle between the radial at the nth line-source radiator (the azimuthal direction of the peak of its beam) and the far-field observation point for which the pattern is being computed.

ϕ_n is the angle from a fixed azimuthal reference on the vehicle to the phase center of the nth line source radiator. It is also the angle to the nth waveguide within the cylindrical lens.

θ_m is the angle from the same fixed reference to the mth elemental radiator at the bottom of the lens.

ψ is the azimuthal angle between the fixed reference and the retrodirection.

γ is the azimuth angle between the retrodirection and the far field observation point.

N is the total number of line-source radiators (and also the number of waveguides at the top of the lens). For the present they will be assumed equally spaced.

---

* It is assumed that there is no mutual coupling between the separate radiators at the same end of the lens.

M is the total number of elemental radiators at the bottom of the lens, (also assumed equally spaced for the present)

R is the effective radius of the line source radiators measured in wavelengths of the pilot signal.

R' is this effective radius measured in wavelengths of the retransmitted signal.

WR is the mean effective radius of the cylindrical geodesic lens.

WRL is the effective length of the cylindrical lens.

$E(\beta)$ is the amplitude function representing the azimuthal radiation pattern of each of the line source radiators. It is assumed to be zero except when $(-\pi/2) \leq \beta \leq (\pi/2)$.

$H(\alpha)$ is the equivalent function associated with the waveguide ends coupling into the top of the geodesic lens.

$G(\alpha)$ is the equivalent function associated with the elemental radiators at the bottom of the lens, each of which is coupled to an individual receiver/amplifier/transmitter.

The azimuthal angle associated with the most direct path between the mth elemental radiator and the nth waveguide can be defined as the first ray and is given by

$$\Delta_{mn1} = 2\pi_p + \theta_m - \phi_n \quad , \tag{1}$$

where $p = 0$, or ± 1 such that $-\pi < \Delta_{mn1} \leq \pi$. The second most direct ray is given by

$$|\Delta_{mn2}| = 2\pi - |\Delta_{mn1}| \tag{2}$$

and will satisfy

$$-2\pi < \Delta_{mn2} \leq -\pi \qquad \text{for } \Delta_{mn1} \text{ positive}$$

and

$$\pi \leq \Delta_{mn2} \leq 2\pi \qquad \text{for } \Delta_{mn1} \text{ negative} \quad .$$

(The sign of Δ_{mni} is of no significance if the elemental radiator patterns are symmetrical and the relativistic effects of the vehicle spin can be neglected.)

Similarly

$$|\Delta_{mn3}| = 2\pi + |\Delta_{mn1}| \quad . \tag{3}$$

By simple geometry (see Fig. 2)

$$\alpha_{mni} = \arctan \frac{\Delta_{mni}}{L} \quad . \tag{4}$$

The net amplitude coupled between the mth amplifier/transmitter and the nth line source waveguide, via the ith path is then given by

$$|A_{mni}| = G(\alpha_{mni})H(\alpha_{mni})\sqrt{\text{Cos } \alpha_{mni}} \tag{5}$$

The electrical length of this ray is given by

$$\epsilon_{mni} = 2\pi RWL \text{ Sec } \alpha_{mni} \text{ radians} \tag{6}$$

The net coupling between the mth elemental radiator and the nth waveguide is then the vector sum:

$$\sum_{i=1}^{3} |A_{mni}| e^{j\epsilon_{mni}} \quad . \tag{7}$$

which holds equally for the pilot beam and the retransmitted signal, provided R' replaces R.

The reradiated powers can now be computed using the same general procedure that was described for the cylindrical-geodesic-lens biconical-horn antenna in the first quarterly report.

Again, the ray length outside the antenna from the distant observation point (located a distance S away and having a relative azimuthal direction γ) to the nth line source radiator is

$$S - R\lambda \text{ Cos } \beta_{n\gamma} = R\lambda\left(\frac{S}{R\lambda} - \text{Cos } \beta_{n\gamma}\right) \quad . \tag{8}$$

The total relative phase difference from each of the M elemental radiators to the distant observation point is

$$\eta_{mni} = 2\pi R(WL \text{ Sec } \alpha_{mni} - \text{Cos } \beta_{n\gamma})^{*} \tag{9}$$

Since each line source radiator has its own azimuthal antenna amplitude function $E(\beta_{n\gamma})$ there will be an additional modification to the amplitude of each vector.

If now a pilot signal is received from direction ψ (*i.e.*, $\gamma = 0$) the signal received at each of the M elemental radiators will be the vector sum.

$$B_m = |B_m| e^{j\Omega_m} = \sum_{n=1}^{N} \sum_{i=1}^{3} E(\beta_{n0}) |A_{mni}| e^{j\eta_{mni}} \tag{10}$$

d. COMPUTATION OF RERADIATION PATTERN

It is again assumed that the conjugate circuitry associated with each elemental radiator reverses the sign of Ω_m on reradiation and that the reradiated power is some function of the received signal amplitude $|B_m|$. (In the particular results presented below, the reradiated amplitudes are all assumed to be equal.)

By using the reverse procedure, the relative signal amplitude apparent at some distant point at an azimuthal angle γ from the pilot signal, which is due to transmission from the mth transmitter via the nth line source radiator and the ith path within the geodesic lens, will be given by

$$D_{mni\gamma} = E(\beta_{n\gamma}) |A_{mni}| e^{j\mu_{mni\gamma}} \tag{11}$$

where

$$\mu_{mni\gamma} = 2\pi R'(WL \text{ Sec } \alpha_{mni} - \text{Cos } \beta_{n\gamma} - \Omega_m) \tag{12}$$

*It will be assumed for the present that the frequencies appearing at each of the elements is identical; hence, $S/(R\lambda)$ is identical for all values of n and can be ignored. Due to vehicle spin, and hence relative Doppler shift, this will not necessarily be true for very large values of S.

The relative field amplitude in any azimuthal direction γ is then given by the vector sum

$$D_\gamma = \sum_{m=1}^{M} \sum_{n=1}^{N} \sum_{i=1}^{3} D_{mni\gamma} \tag{13}$$

This value is more appropriately designated in dB by

$$F_\gamma = 20 \log_{10} |D_\gamma| \tag{14}$$

This value has been computed for several points at or around the retrodirection and some of these results are presented below.

e. DETERMINATION OF ANTENNA AZIMUTHAL GAIN

As was done in the first quarterly report for the biconical-horn antenna, the peak power of the reradiation pattern is compared with the average power radiated in all directions. It was not possible to reuse Methods 1 and 2, requiring integration of the reradiation patterns, since patterns were computed only over a small arc, and sometimes just a single point, rather than for all azimuthal directions. The gain values previously obtained by these two methods were in all cases within 0.06 dB of each other, and in each case about 0.2 dB higher than the value obtained by Method 4. This latter method involved the computation of the total energy radiated by the elemental radiators within the geodesic lens, and then made the assumption that this was all radiated into space without reflection loss from the discontinuities within the antenna. The average value of the resultant radiation intensity is designated by Q (in dB). Such a condition is easier to realize in the case of the biconical-radiator antenna than in this discrete-line-source antenna where the energy must be coupled, without loss, from a TEM line into adjacent waveguides. The computed value of gain resulting from this technique should be reasonably accurate, if perhaps a little optimistic.

It has also been assumed that each radiating element is optimally matched to its appropriate transmitter at all times. This is equivalent to neglecting mutual coupling which, in practice, might vary with vehicle rotation.

f. RESULTS OF COMPUTATION

i. Introduction

Some results of a series of computations are shown in the following figures.

Figure 3 is the computed pattern used as the reference for most of the rest of the computations, and has the following values of coefficients.

$R = 10{,}000$ $\qquad$ $E(\beta) = 10^{-24(R\beta/N)^2}$

$R'/R = 1.000$ $\qquad$ $G(\alpha) = 10^{-24(WR\alpha/N)^2}$

$W = 1.00$ $\qquad$ $H(\alpha) = 10^{-24(WR\alpha/cM)^2}$

$L = 3.00$ $\qquad$ $\psi = 2$ degrees

$M = 40$ $\qquad$ $c = 2$

$N = 80$

The fact that the retrodirection is 2 degrees from the zero reference of the antenna (which is an axis of symmetry) accounts for the computed pattern being asymmetrical. It should be noted that although points have been plotted every one degree this is not close enough to make a reliable interpretation of the correct pattern shape, including null depths, *etc.* Consequently, the computed points have been joined by straight lines.

It should also be noted that each point represents the vectoral summation of $3 \times M \times N/2 = 4800$ field intensities, each of which involves the product of at least four computed quantities.

The 3-dB beamwidth as well as the gain in dB, computed by subtracting the value of Q from the computed signal intensity in the retrodirection, is shown on Fig. 3 (as well as on subsequent patterns). Using the same argument as used in the first quarterly report, the maximum possible theoretical gain of this antenna averaged over all azimuthal pointing directions is postulated as

$$P = 10 \log_{10} M = 16 \text{ dB} \qquad (15)$$

The compared value of gain, 14.66 dB, thus appears quite reasonable.

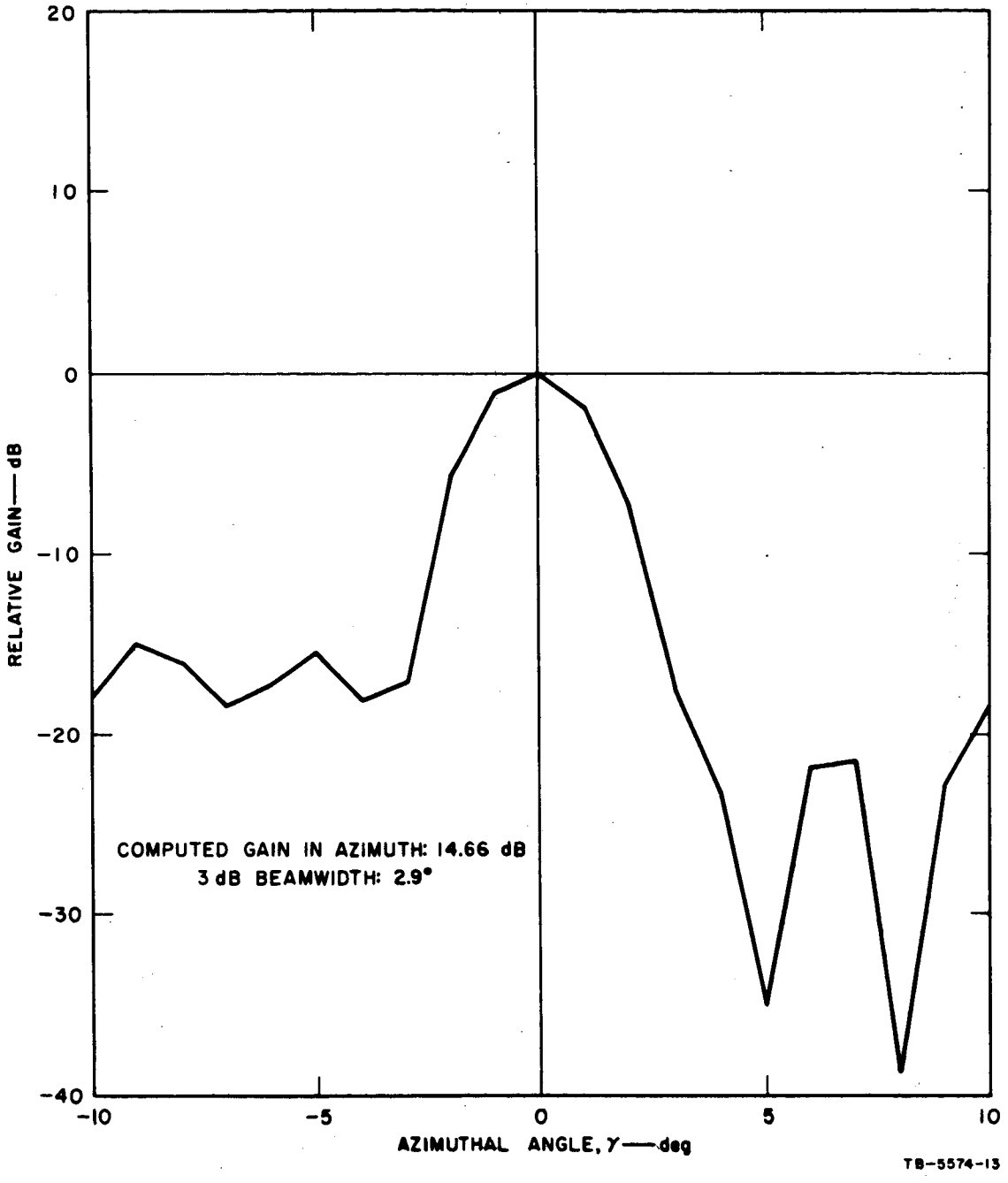

FIG. 3 BASIC ANTENNA PATTERN USED AS REFERENCE

ii. Variation in Max ERP with Antenna Spin

Figure 4 shows the computed value of gain in the retrodirection as the antenna is rotated through $360/M$ degrees which represents one cyclical period for this configuration. It can be seen that the average computed value of gain is about 15.0 dB and it varies by nearly ±0.5 dB. This variation could be very undesirable and compares unfavorably with the similar computations made for the biconical-horn version, where no gain variation was observed (for two computed values of maximum gain).

iii. Variation in ERP with Change in Frequency

The gain in the retrodirection was computed for an antenna with the same characteristics as the reference antenna except that the operating frequency (which again was the same for receiving as for transmitting) was increased by nearly 0.1 percent in increments of 0.01 percent. The ERP, or gain, was found to decrease by 0.06 dB in an apparently linear manner. Since the gain of any antenna would normally *increase* when the frequency is increased it is assumed that the small decrease observed is part of a superimposed cyclical variation.

iv. Variation in ERP as Retransmitted Frequency is Changed

It is almost certain that the receive and transmit frequencies will be different for any retrodirective system; and this frequency separation is likely to be at least a few percent.

If one antenna is used for receiving the pilot beam and each elemental receiver of this antenna is coupled to the corresponding transmitter of a separate transmitting antenna, which has all dimensions exactly scaled in the ratio of the operating wavelengths, then this frequency difference is not very important. If, on the other hand, the same antenna is used, together with simple phase-conjugating networks, then the frequency separation will definitely cause "defocusing", which will reduce the ERP in the retrodirection.[2] If more complex conjugating circuits are employed, involving signal frequency multiplying and dividing, then this defocusing can be removed.[3] Such a scheme is discussed under Task III (Part C below).

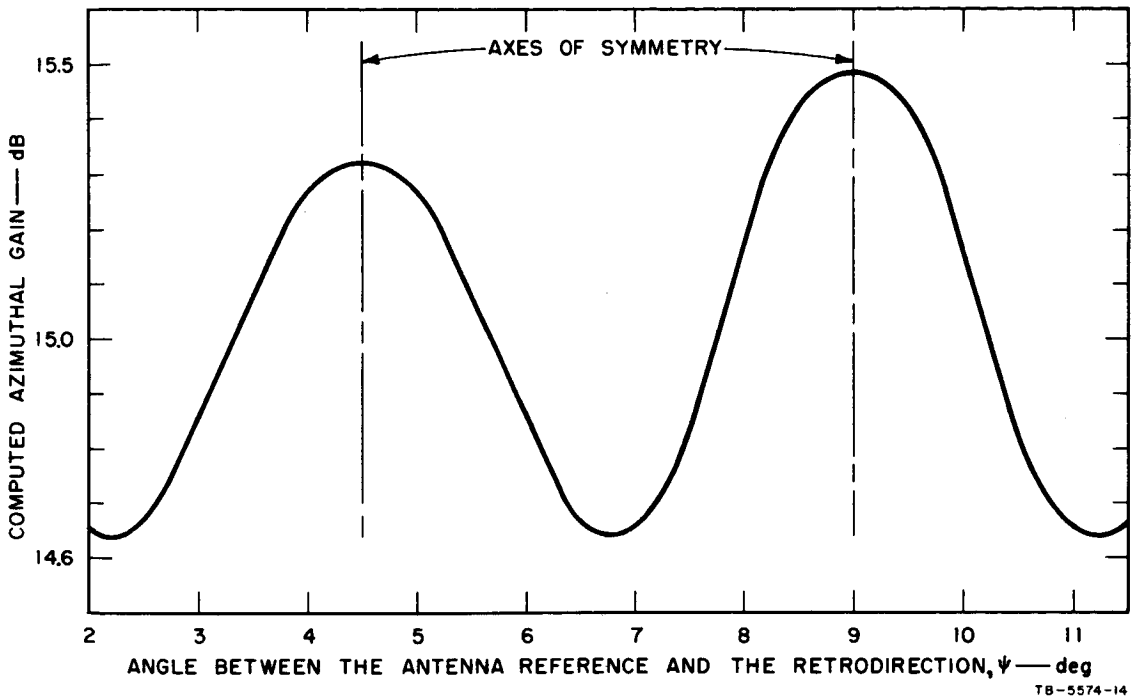

FIG. 4 COMPUTED GAIN IN THE RETRODIRECTION AS A FUNCTION OF A ROTATION OF THE ANTENNA

To determine the effect of this defocusing, antenna gains were computed as a function of retransmitted frequency. The gain in the retrodirection was found to fall by nearly 6 dB for a retransmitted frequency increase of 5 percent. Three patterns, one of which is the reference pattern shown in Fig. 3, are shown in Fig. 5. The gain in each case is with respect to an omni-azimuthal element of equal elevation beamwidth. Figure 6 shows the azimuthal gain in the retrodirection with respect to the theoretical maximum value of 16 dB. The fact that the retrodirection was taken as 2 degrees from an axis of symmetry of the antenna no doubt accounts for the nonmonotonic form of Fig. 6 and the fact that the maximum ERP is not always in the retrodirection (see Fig. 5).

v. Variation in the Number of Line-Source Radiators, N

Figure 7 shows a set of patterns for three similar antennas. The number of line-source radiators, N, is varied from 40 to 80. The elemental radiation pattern is also automatically modified, as can be seen from the definition of $E(\beta)$ and $H(\alpha)$. The reference pattern of Fig. 3 ($N = 80$) is again reproduced.

It can be seen from Fig. 7 that the gain actually increases as the number of line-source radiators is reduced (although the number of elemental transmitters, M, has been kept constant at 40). By interpolation from Fig. 4 it can be estimated that about 0.4 dB of this apparent increase in gain of nearly 1.0 dB can be attributed to the cyclical variations of the max ERP with ψ. There is at present no explanation for the remaining one-half dB.

The inference is that there is no point in increasing the number of line-source radiators and hence the complexity of the antenna, in order to improve antenna gain. It is quite likely however that fewer radiators will lead to larger gain variation with spin, but no direct measurements have yet been made to confirm this.

vi. Variation in the Elemental Radiation Patterns

In all the results presented above, the number of elemental radiators, M, has been kept constant at 40. The radiation pattern of each of these elements denoted by

$$G(\alpha) = 10^{-24(WR\alpha/cM)^2}$$

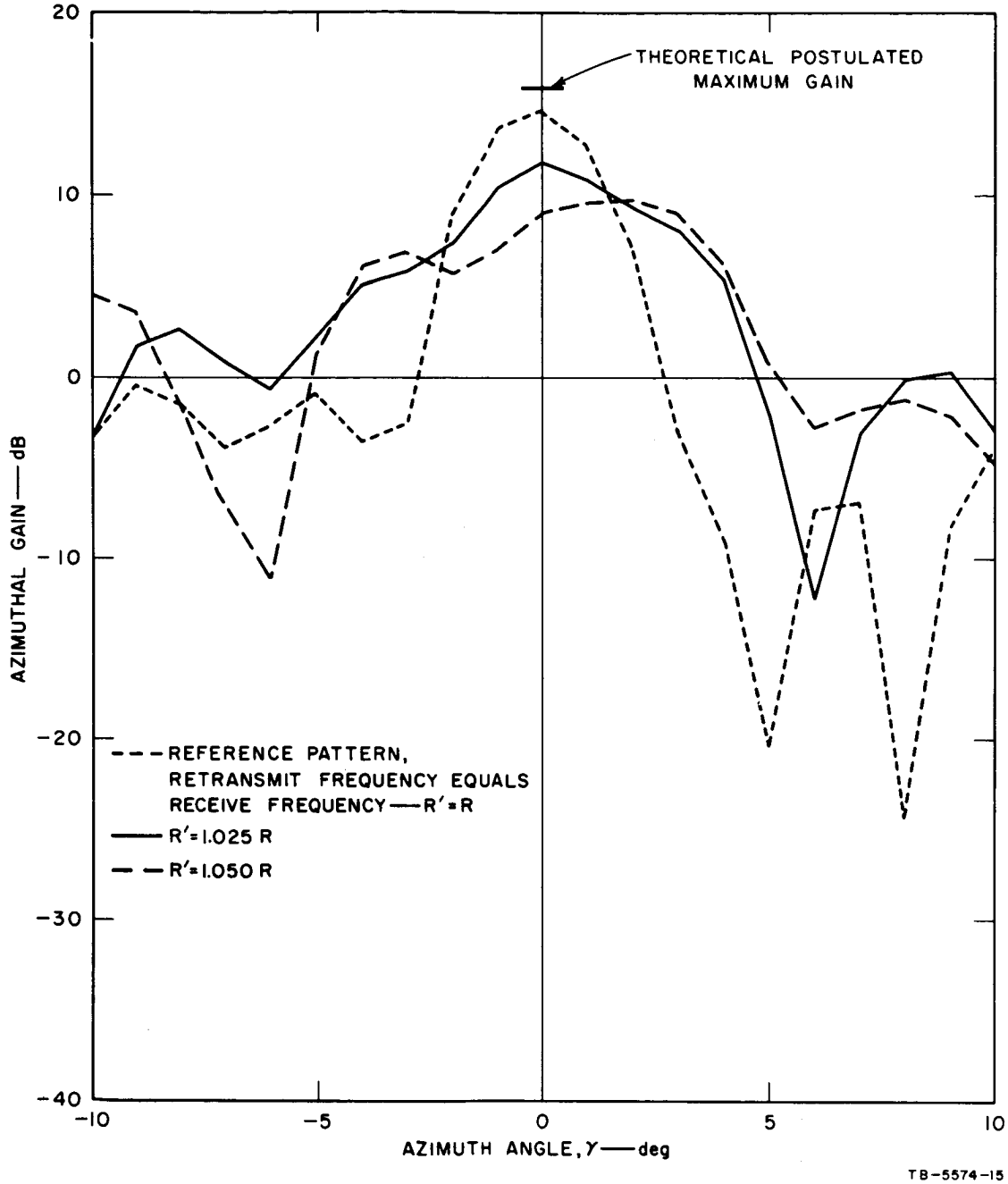

FIG. 5 BEAM SHAPES AS A FUNCTION OF THE RETRANSMITTED FREQUENCY: RECEPTION AND TRANSMISSION USING THE SAME ANTENNA

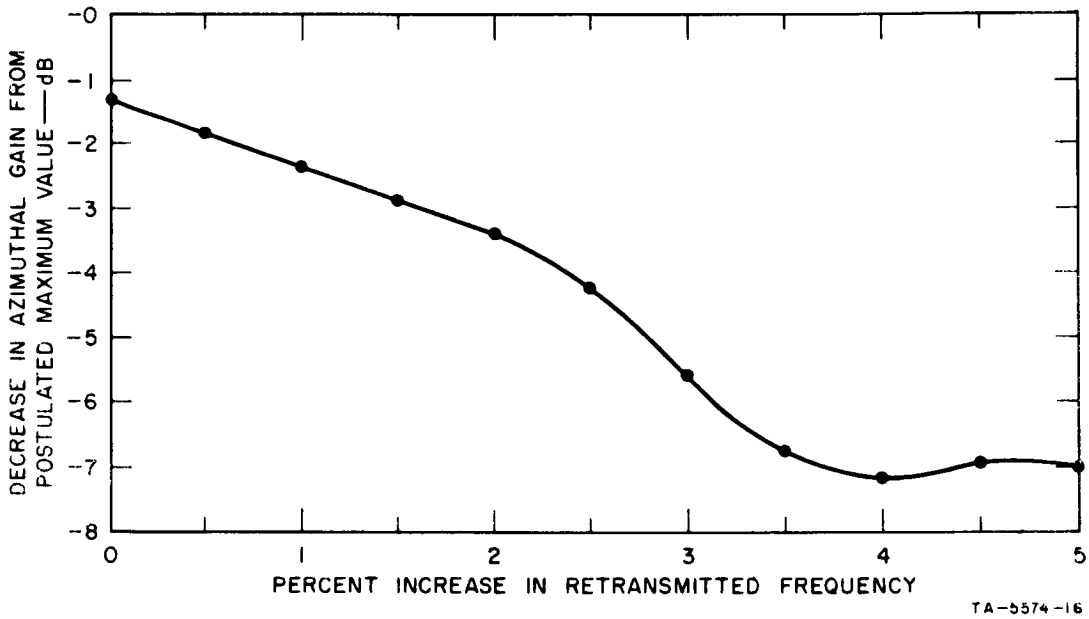

FIG. 6 DECREASE IN GAIN WITH INCREASE OF R'

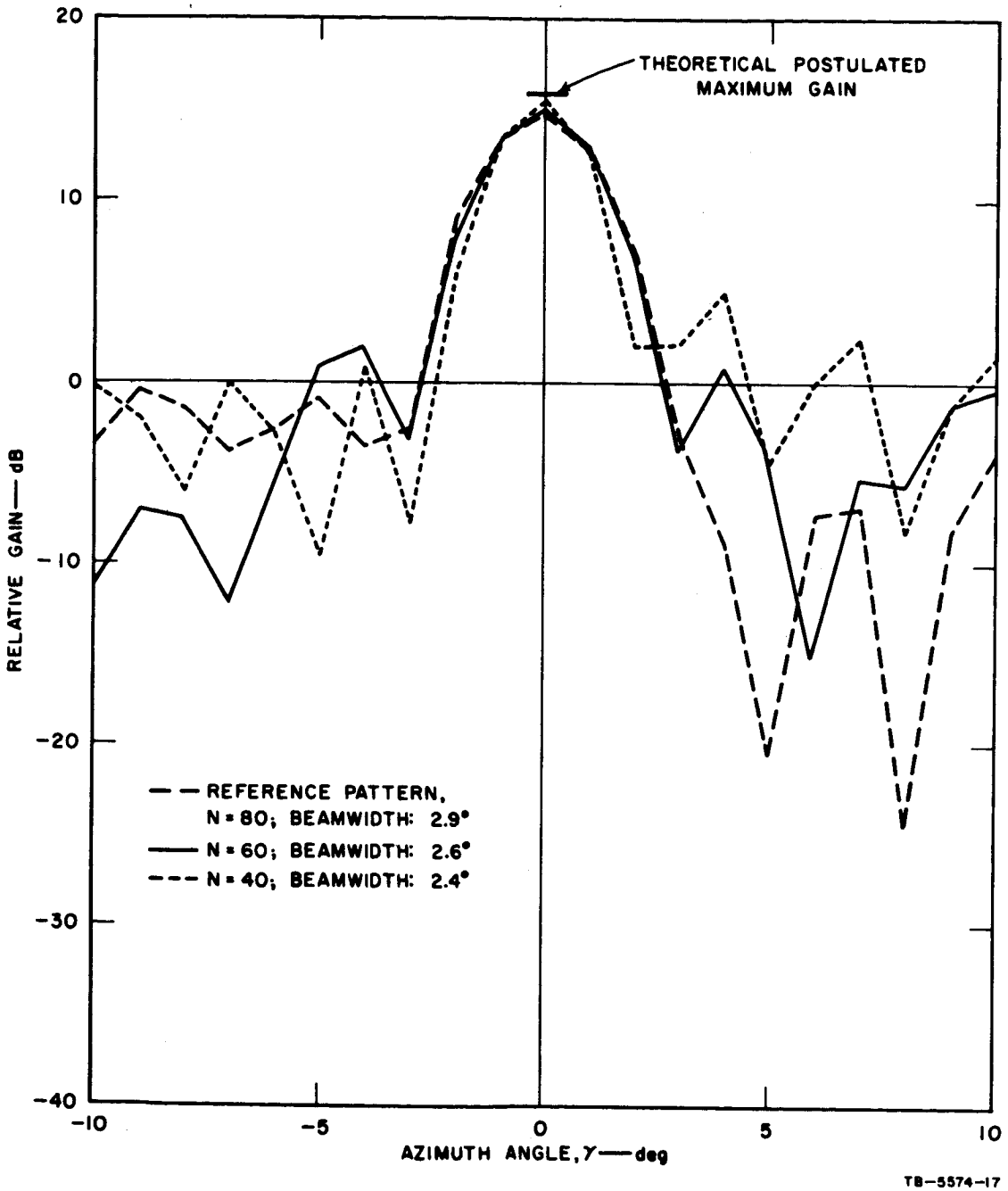

FIG. 7 EFFECT OF CHANGING VALUE OF N ON THE AZIMUTHAL GAIN

has also been kept constant (except for minor variations in R as the frequency was varied). The constant $1/C$ is the proportion of available arc at the bottom of the cylindrical lens that is used for each elemental radiator. In the above results c has had the value 2, indicating that twice as many similar elemental radiators could have been fitted into the space available. For such an arrangement, *i.e.*, $M = 80$, the mutual coupling between adjacent radiators would be considerably higher, and previous results[1] have indicated that the antenna gain *per transmitter* would not increase and may very well decrease. The larger number of transmitters would however increase the ERP for the same total power input at the expense of more receiver/amplifier/transmitters.

The effect of this parameter c was investigated by assigning it different values and computing the gain in the retrodirection. The following results were obtained.

for c =	1.0	1.5	2.0
gain =	14.58	14.88	14.66 dB

Since the accuracy of the computed gain is only about 0.5 dB the minor differences between these values of gain are considered insignificant. Thus it would appear that for a given diameter antenna and given number of transmitting elements the efficiency with which the available aperture within the lens is used is not very significant.

vii. Characteristics of a Smaller Antenna

Continuing the general investigation of the various antenna parameters, the linear dimensions as well as the value of M and N were halved. Computed patterns for the cases of $N = 20$ and 40 are shown in Fig. 8. It can be seen that the antenna with the smaller number of line-source radiators gives a gain three-quarters dB higher than the other one. This is consistent with the results shown in Fig. 7. The beamwidth for the higher gain antenna is also narrower but a very high side lobe level is apparent.

2. Circular Array of Omnidirectional Elements

a. Introduction

One form of retrodirective array that might be suitable for use with a spin-stabilized vehicle consists of line-source elements mounted at one end of a cylindrical vehicle, as shown in Fig. 9. The beamwidth

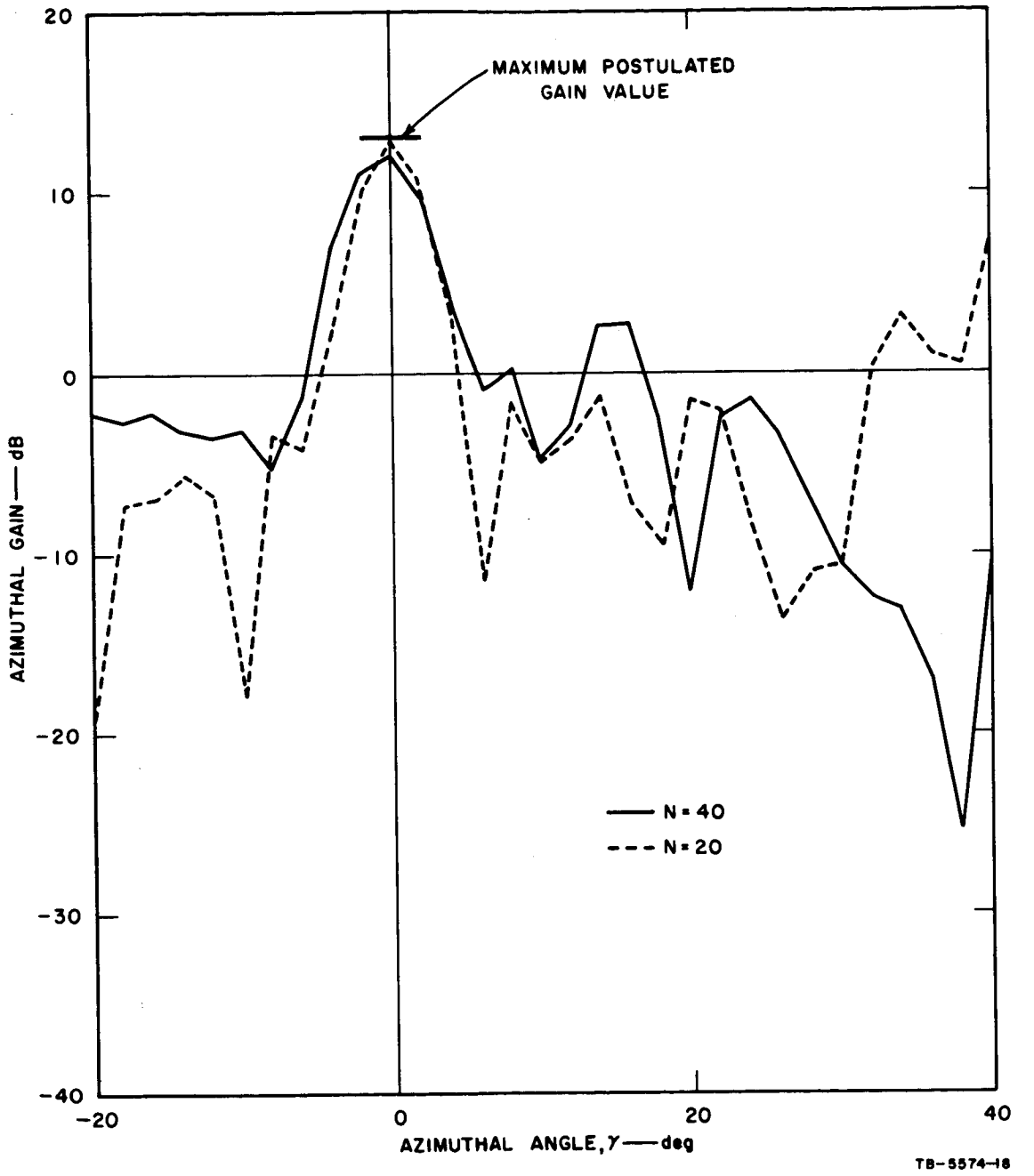

FIG. 8 COMPUTED PATTERN FOR TWO VALUES OF N USING A 10λ DIAMETER ANTENNA

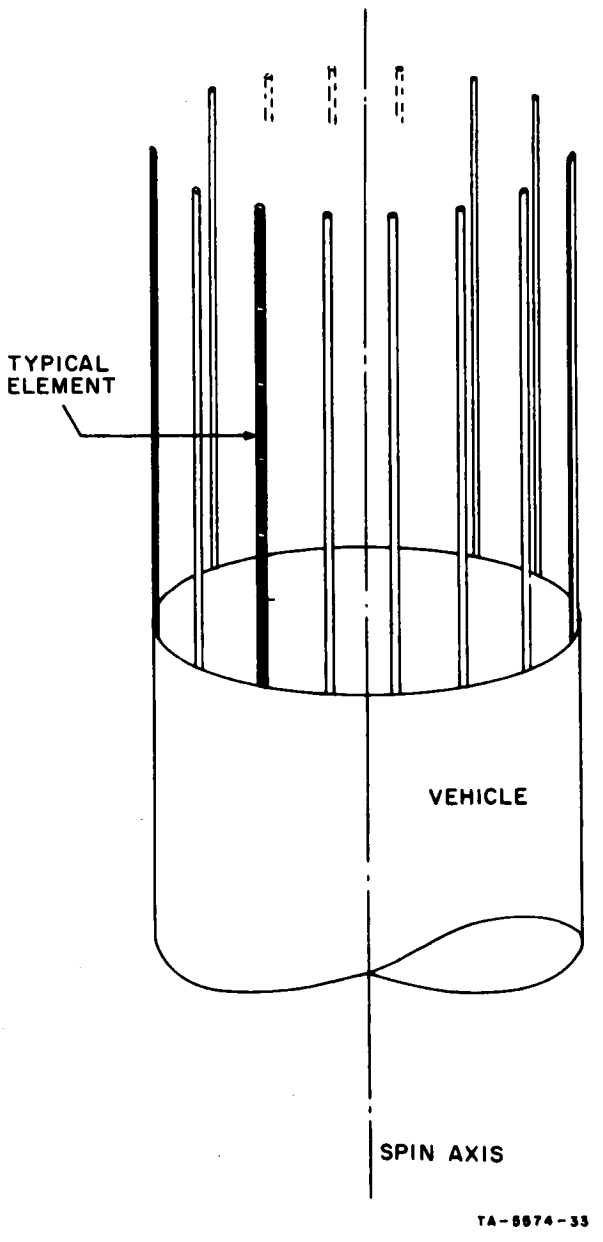

FIG. 9 OMNIAZIMUTH-ELEMENT CIRCULAR ARRAY ON THE END OF A CYLINDER

of each element in a plane through the vehicle spin axis would be relatively narrow, as determined by the length of the element in wavelengths. Again, orientation of the beam in this plane would be provided by spin stabilization of the vehicle. Each element would have a very broad beam in the plane perpendicular to the spin axis, but the array as a whole would have a narrow beam in this plane. Orientation of the array beam would be provided by retrodirective circuitry connected to each line-source element.

For purposes of the present analysis, it is assumed that each element has an omnidirectional pattern in the plane perpendicular to the spin axis, and that mutual coupling and shadowing of one element by another will have negligible effect on the array pattern. In actual practice, the element diameter would probably be large enough compared to the wavelength and compared to the interelement spacing that shadowing would not be completely negligible. Also the element pattern for an element in the array would not be exactly omniazimuthal, due to mutual coupling, even if the element pattern was omniazimuthal for a single element in free space. An additional effect of mutual coupling would be to make the input impedance of each element a function of its location in the array. Therefore, the assumption of equal current flowing on each element, which is used in calculating the radiation patterns, is not equivalent to having equal power radiated from each element.

Analyses of circular arrays of omnidirectional radiators are available in the literature, but the numerical results that have been presented are for smaller numbers of elements and for smaller array diameters than are of interest for the present application. In this section of the report, properties of circular arrays will be reviewed, and some calculated patterns will be presented for arrays of 30, 60, and 90 elements on a 20-wavelength diameter. Also, the gain modulation as arrays of 60 and 61 elements rotate will be given.

b. Pattern Shape

Whether a circular array of elements radiates a broad or a pencil beam, as well as the direction of a pencil beam, depends on the amplitude and phase of the current in each element. Of primary interest in the present application is a pencil beam radiated in the plane perpendicular to the spin axis of a space probe. It will be convenient here to refer to this plane as the *azimuth plane*. The proper current

distribution to form a pencil beam from a circular array has been considered in detail by several authors,[4-7] and thus need not be derived in detail here. Rather, a few of the fundamental equations will be given, and some calculated patterns shown. The primary reason for considering the pattern shape and side lobe behavior is to understand why the gain of the array changes with array orientation, and to establish how many elements are required to keep the gain reasonably constant. The form of the equations presented will closely follow Knudsen.[4]

Referring to Fig. 10, it is readily seen that in order to launch a plane wave the proper current phase lag in the kth element in an array of N identical omniazimuth elements equally spaced around a circle of radius R is given by

$$\psi_k = 2\pi R \cos\left(\frac{2\pi k}{N} - \phi_i\right), \quad k = 1, 2, \ldots, N.^* \tag{16}$$

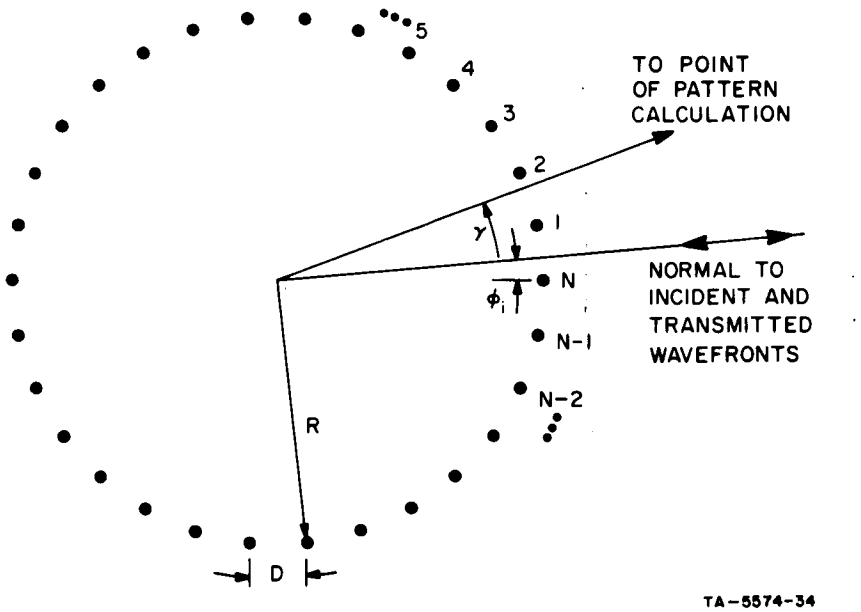

FIG. 10 DEFINITION OF RING-ARRAY PARAMETERS

* The symbols used for the discussion of a particular antenna type will in general be applicable only to that type.

Here R is measured in units of wavelength, and the phase is in radians. The phase reference is the center of the circle. The angle ϕ_i defines the orientation of the array with respect to the incident ray along which the transmitted beam is to be pointed (the retrodirection). Equation (16) also gives, of course, the relative phase *lead* of the current induced in each element by a plane-wave incident pilot signal, assuming mutual coupling between elements to be insignificant. Changing phase *lead* for an incident signal to phase *lag* of a transmitted signal is another way of stating that a phase conjugate network is required on each element of a retrodirective array.

The far-field amplitude pattern is obtained by summing the contribution of the individual elements in the array. For unity current amplitude in each element, the resultant amplitude pattern is proportional to[4]

$$E = \sum_{k=1}^{N} \exp\left\{ j 2\pi R \left[\cos\left(\frac{2\pi k}{N} - \phi_i - \gamma \right) - \cos\left(\frac{2\pi k}{N} - \phi_i \right) \right] \right\} \qquad (17)$$

For the special case of an even number of elements, $\exp(jx)$ can be replaced by $\cos(x)$.[8] To reduce the time for a digital computer to calculate the patterns, Eq. (17) was rewritten using a trigonometric identity to obtain Eq. (18).

$$E = \sum_{k=1}^{N} \exp\left[j 4\pi R \sin\frac{\gamma}{2} \sin\left(\frac{2\pi k}{N} - \phi_i - \frac{\gamma}{2} \right) \right] . \qquad (18)$$

The computer evaluates trigonometric functions using a many-termed power series, which is relatively time consuming compared to operations of multiplication and addition. Thus even more computer time was saved by using the following recursion relations.

$$\frac{2\pi k}{N} - \phi_i - \frac{\gamma}{2} = \left[\frac{2\pi(k-1)}{N} - \phi_i - \frac{\gamma}{2} \right] + \frac{2\pi}{N} \qquad (19)$$

thus

$$\sin\left(\frac{2\pi k}{N} - \phi_i - \frac{\gamma}{2}\right) = \sin\left[\frac{2\pi(k-1)}{N} - \phi_i - \frac{\gamma}{2}\right]\cos\frac{2\pi}{N} + \cos\left[\frac{2\pi(k-1)}{N} - \phi_i - \frac{\gamma}{2}\right]\sin\frac{2\pi}{N} \tag{20}$$

$$\cos\left(\frac{2\pi k}{N} - \phi_i - \frac{\gamma}{2}\right) = \cos\left[\frac{2\pi(k-1)}{N} - \phi_i - \frac{\gamma}{2}\right]\cos\frac{2\pi}{N} - \sin\left[\frac{2\pi(k-1)}{N} - \phi_i - \frac{\gamma}{2}\right]\sin\frac{2\pi}{N} \tag{21}$$

for $k = 1, 2, \ldots, N$.

That is, to find

$$\sin\left(\frac{2\pi k}{N} - \phi_i - \frac{\gamma}{2}\right)$$

for all values of k, it was necessary to use the power series for the trigonometric functions to evaluate only

$$\sin\left(-\phi_i - \frac{\gamma}{2}\right), \quad \cos\left(-\phi_i - \frac{\gamma}{2}\right)$$

$$\sin\frac{2\pi}{N}, \quad \text{and} \quad \cos\frac{2\pi}{N} .$$

Some characteristics of the radiation patterns of circular arrays having different numbers of elements on the same diameter circle are illustrated in Figs. 11 through 13.* For each of these figures the array diameter is 20 wavelengths, and the number of elements is 30, 60, and 90 for the respective figure. It is seen that the main beam and the

* These patterns were machine plotted, connecting the computed points that are spaced every degree by straight lines. The finite point spacing does not show the true depth of the nulls, or the peaks of some lobes.

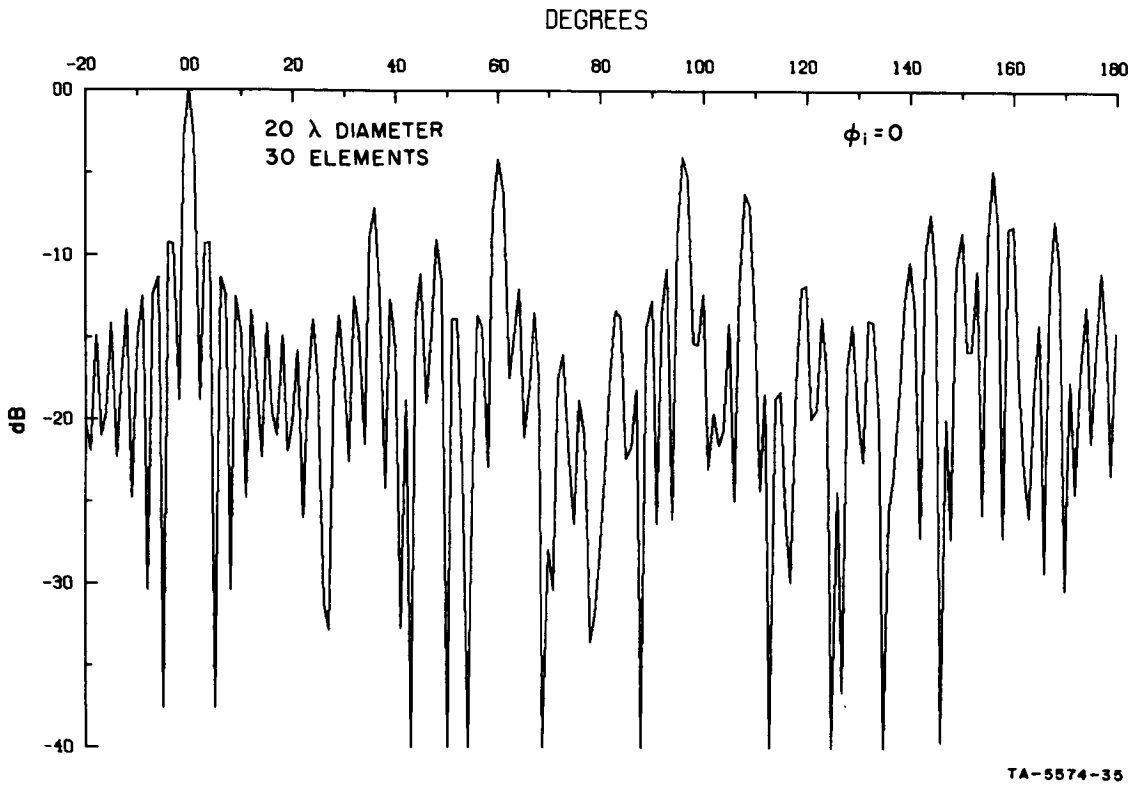

FIG. 11 COMPUTED PATTERN OF A 20-λ DIAMETER, 30-ELEMENT CIRCULAR ARRAY

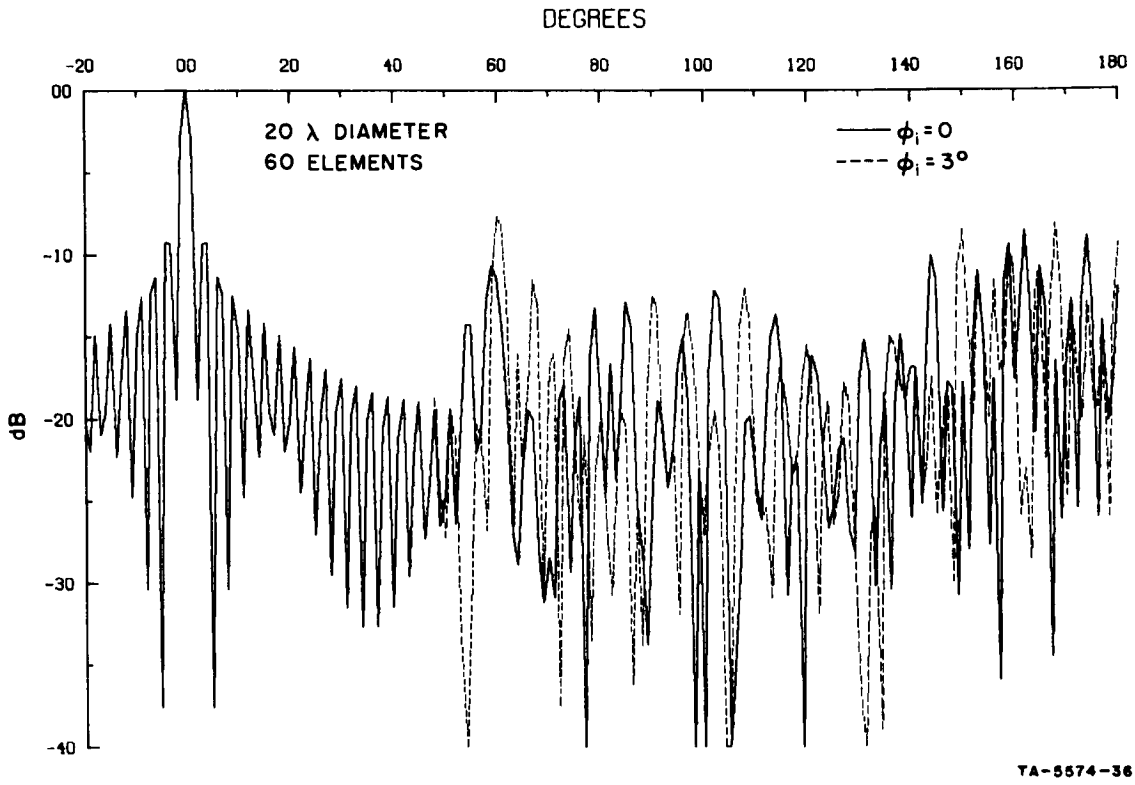

FIG. 12 COMPUTED PATTERN OF A 20-λ DIAMETER, 60-ELEMENT CIRCULAR ARRAY

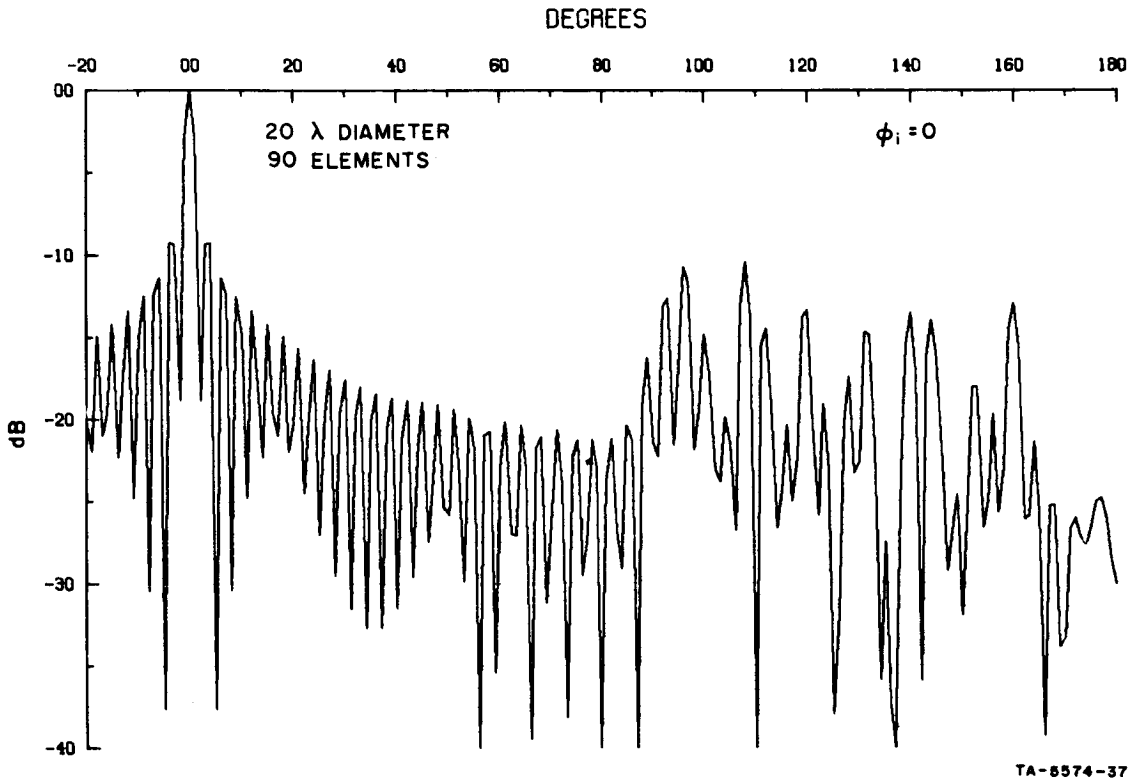

FIG. 13 COMPUTED PATTERN OF A 20-λ DIAMETER, 90-ELEMENT CIRCULAR ARRAY

first several side lobes are identical in the three figures. Also note that the side lobes fall off in a well-behaved manner out to a certain angle, beyond which the lobe height increases significantly and the lobe shape becomes less systematic. The more elements there are in the array, the further out in angle are the side lobes well behaved.

These characteristics of the patterns from circular arrays can be explained by rewriting Eq. (17) as a series of Bessel functions.[4]

$$E = J_0\left(4\pi R \sin\frac{\gamma}{2}\right) + 2\sum_{p=1}^{\infty} J_{pN}\left(4\pi R \sin\frac{\gamma}{2}\right)\cos\left[pN\left(\frac{\gamma}{2} + \phi_i\right)\right] \tag{22}$$

for N even, and

$$E = J_0\left(4\pi R \sin\frac{\gamma}{2}\right) + 2\sum_{p=1}^{\infty} J_{2pN}\left(4\pi R \sin\frac{\gamma}{2}\right)\cos\left[2pN\left(\frac{\gamma}{2} + \phi_i\right)\right]$$

$$+ j2\sum_{p=0}^{\infty} J_{(2p+1)N}\left(4\pi R \sin\frac{\gamma}{2}\right)\sin\left[(2P+1)N\left(\frac{\gamma}{2} + \phi_i\right)\right] \tag{23}$$

for N odd. Here $J_k(x)$ is the Bessel function of the first kind and of order k. The leading term, which involves the J_0 function, is the amplitude pattern resulting if the circular array consisted of an infinite number of identical omniazimuth elements. The summations can be considered as correction terms to account for the fact that the number of array elements is finite. The main lobe and the first several side lobes in the patterns of Figs. 11 through 13 are given by the J_0 term of Eq. (22). Where the side lobes no longer decrease monotonically is where the first term in the correction series becomes important.

The first correction term that becomes significant in both Eqs. (22) and (23) is a $J_N(x)$ function, where the order N is the same as the number of elements in the array. For an array 20 wavelengths in diameter, practical numbers of elements might lie in the range 50 to 100, thus the correction series involve Bessel function of high order. It is characteristic of Bessel functions of the first kind and of high order that they have small value for arguments small compared to the order. As the argument approaches the order, the function increases rapidly to a positive peak, and then becomes oscillatory eventually approaching a decaying sinusoidal waveform. For discussion of these

functions see, for example, Jahnke and Emde,[9] and Watson.[10] The location of the first positive peak of the function $J_N(x)$ is given approximately by[11]

$$x \approx N + 0.808 N^{1/3} \tag{24}$$

That is, the location of the highest of the first spurious side lobes of the array pattern would be given by

$$\sin \frac{\gamma}{2} \approx \frac{N + 0.808 N^{1/3}}{4\pi R} \quad . \tag{25}$$

The exact location of the highest spurious side lobe will also depend on the factor $\cos N(0.5\gamma + \phi_i)$ in Eq. (22), or $\sin N(0.5\gamma + \phi_i)$ in Eq. (23), and on the side lobes of the J_0 leading term.

Equation 25 gives the location of the first spurious side lobes in terms of the number of elements and the array radius. Based on experience with the more familiar linear arrays, a more fundamental relationship for spurious side lobes might be expressed in terms of the element-to-element spacing. (In the case of linear arrays, the spurious side lobes are referred to as diffraction or grating-lobes.) If we define D as the element-to-element spacing measured around the circumference of the array*, and measured in units of wavelength, then

$$D = \frac{2\pi R}{N} \text{ radians} \quad . \tag{26}$$

Defining γ_{sl} as the angle at which the highest spurious side lobe due to the first correction term in Eqs. (22) and (23) can occur, we have

$$\sin \frac{\gamma_{sl}}{2} \approx \frac{1}{2D} + \frac{0.404}{(2\pi R)^{2/3} D^{1/3}} \quad . \tag{27}$$

* The circumferential spacing D defined here is nearly the same as the spacing measured along the cord connecting adjacent elements when the number of elements is large. The two ways of measuring spacing are equal to the same accuracy as the approximation $\sin(\pi/N) \approx \pi/N$, where N is the number of elements in the array.

Equation (27) has been plotted in Fig. 14 for several values of array diameter. It is seen that the angle at which the first spurious side lobes can occur is rather insensitive to the array diameter.

The side lobes far beyond the first spurious lobes require additional terms in the correction series of Eqs. (22) and (23). For the array diameters and numbers of elements that would be practical for retrodirective arrays on space probes, however, only a few terms of the correction series need be evaluated. As an example, for a 20-wavelength diameter array with as few as thirty elements, only the J_{30}, J_{60}, J_{90}, and J_{120} functions would have significant amplitude. (For sixty elements on the same diameter, only the J_{60} and J_{120} correction terms would have to be taken into account.) Taking $4\pi R = 40\pi = 125.7$, the first positive peaks in the correction series in Eqs. (22) and (23) occur at 30.0 degrees for the J_{30} term, at 60.3 degrees for J_{60}, at 96.2 degrees for J_{90}, and at 161.2 degrees for J_{120}.

c. SIGNAL AMPLITUDE-MODULATION DUE TO ARRAY ROTATION

Having discussed in some detail the shape of the array radiation pattern, let us now consider the effect that the pattern shape has on the gain (directivity) at the peak of the main beam. Referring back to Eqs. (22) and (23), we see that the shape of the main beam and the first several side lobes is determined by a J_0 function that is independent of the array-orientation angle ϕ_i defined in Fig. 10. The correction series, which influence the farout side lobes, are functions of the array-orientation angle ϕ_i. Thus, as a spin-stabilized space probe with a circular retrodirective array rotates, the side lobes of the array will change as a function of time. An example was shown by the solid and dashed patterns of Fig. 12. As the amount of power radiated into the side lobes changes with time, the gain at the peak of the main beam will change also. This will result in amplitude modulation of the transmitted signal at a frequency related to the rotation rate of the space probe and the number of array elements.

The computer program of Eq. (18) has been used to calculate the directivity of some arrays as a function of array orientation. The directivity at the beam peak was determined from the values of the amplitude pattern, $E(\gamma)$, by numerically integrating

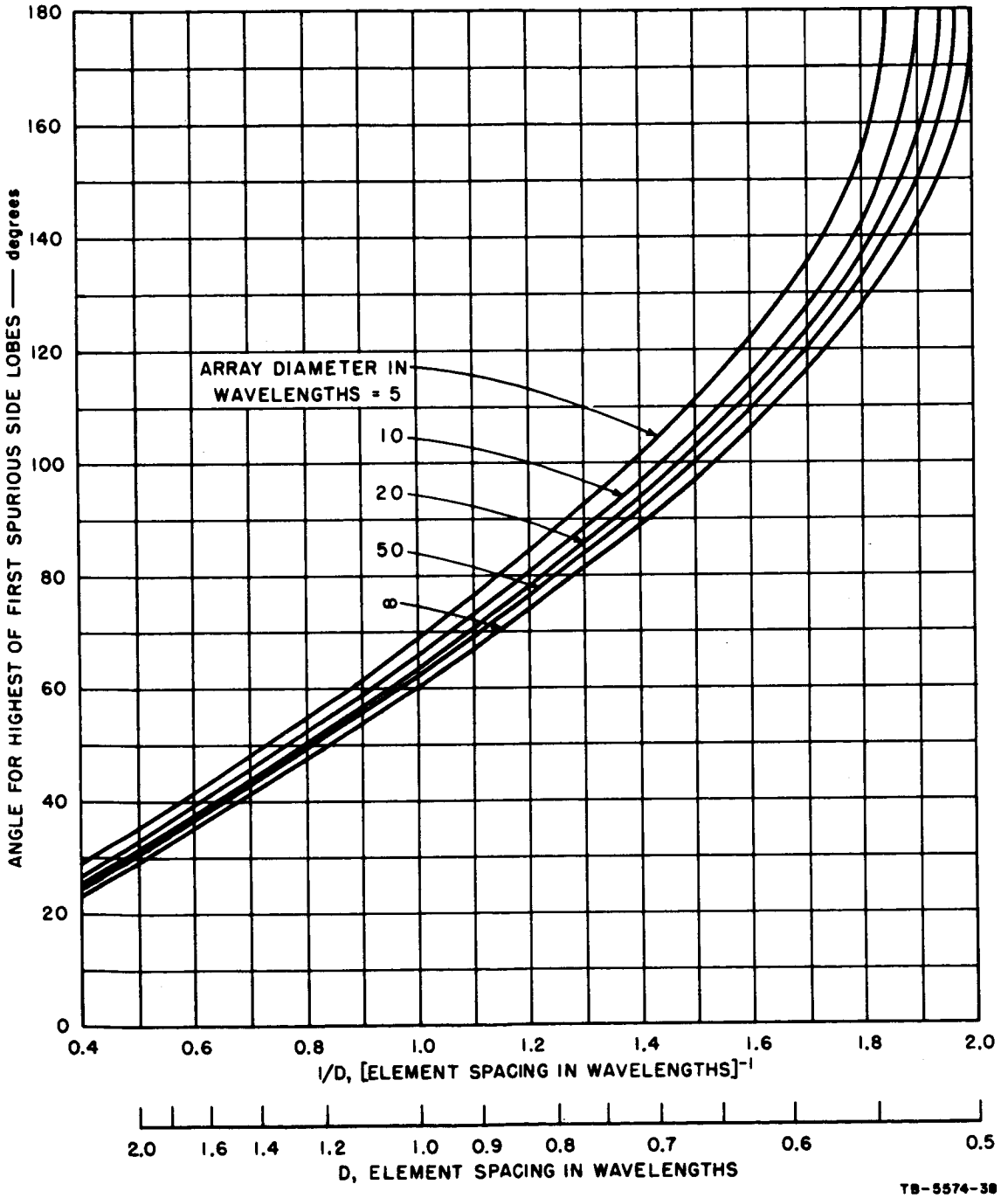

FIG. 14 SPURIOUS-LOBE LOCATION AS A FUNCTION OF ELEMENT SPACING

$$G = \frac{2\pi E_{max}^2}{\int_0^{2\pi} E^2(\gamma)\, d\gamma} \tag{28}$$

An increment of one degree was used for the angle, and Simpson's rule was used to perform the numerical integration.* The factor 2π rather than 4π occurs here since the integration is performed only over the azimuth plane rather than over all space. To find the total directivity of an actual array, the pattern in all directions would have to be taken into account.

Thus far, only 60- and 61-element arrays with 20-wavelength diameter have been used for complete modulation calculations. For the 60-element array, the directivity was found to have an 0.24-dB peak-to-peak ripple, varying in approximately a sinusoidal manner as a function of ϕ_i. The minimum azimuthal directivity of 15.63 dB occurred at ϕ_i = 0, 6, 12, ..., degrees, and the maximum of 15.87 dB occurred at ϕ_i = 3, 9, 15, ... degrees. In this particular case, the minimum directivity occurred when the beam direction was lined up with an array element, and the maximum gain occurred when the beam direction was midway between array elements. For the 61-element array, the directivity had a peak-to-peak ripple of only 0.01 dB as ϕ_i was varied. The minimum directivity of 15.88 dB occurred at ϕ_i = 0, $180/N$, $360/N$, ... degrees. The round-off of the computer printout to the nearest 0.01 dB did not permit determination of the location of the maximum directivity, but the symmetry of the results implied that maximum directivity occurred at odd integer multiples of $90/N$ degrees.

Some calculations that are in progress for other numbers of array elements have shown that the minimum directivity does not in general occur for ϕ_i = 0. Based on the calculations that have been completed to date, plus examination of Eqs. (22) and (23), it is possible to make some general statements regarding the periodicity of the directivity modulation. For an even number of elements, the directivity modulation will be at a frequency

$$f_m = Nf_r \text{ Hz} \tag{29}$$

* The calculated directivity was printed out by the computer to the nearest 0.01 dB. The error introduced by the one-degree spacing of calculated pattern has not been precisely determined. An indication of the accuracy achieved is given by the fact that decreasing the sampling interval for a few 20-wavelength diameter arrays changed the calculated directivity by no more than 0.13 dB in going from 2- to 1-degree increments, and no more than 0.01 dB in going from 1.0- to 0.5-degree increments.

and its harmonics, where f_r is the spin rate of the space probe in revolutions per second. For an odd number of elements, the same equation applies in general. For the special case where an odd number of elements is sufficiently large that only the first correction term in Eq. (23) is significant, however, only the even harmonics of Eq. (29) will be present in the directivity modulation. (As specific examples, for a 60-element array, $f_m = 60f_r$, but for a 61-element array, $f_m = 122f_r$, plus harmonics.)

The fact that the 61-element array gave much lower directivity modulation than did the 60-element array deserves special note. This was anticipated based on the fact that previous investigations dealing with smaller circular arrays had found that an odd number of elements was better than an even number.[4,12,13] For a large number of elements, such as 60 or 61, the pattern does not appear by visual inspection to be a significantly better approximation to a J_0 function for an odd number of elements than for an even number, in contrast to the results for small numbers of elements.[4] What is important here, however, is not obtaining a specific pattern shape, but having the amount of power radiated into the side lobes relatively independent of the array orientation.

Note that, for both Eqs. (22) and (23), the first correction term involves the same function, (except one has a cosine factor and the other a sine factor). The significant difference between Eqs. (22) and (23) is that for N even, the correction terms add either in or out of phase with the leading J_0 term, but for N odd the first correction term adds in quadrature to the leading J_0 term. At any given angle γ, the correction term will sometimes be positive and sometimes negative, depending on the array orientation ϕ_i. Since the correction term is of the same order of magnitude as the side lobes of the J_0 function, adding or subtracting the two terms in phase can produce a much larger change in magnitude of the resultant than does adding the two terms in quadrature. Stated in symbols,

$$\left|\frac{a + b}{a - b}\right| > \left|\frac{a + jb}{a - jb}\right| , \qquad (30)$$

where a represents the J_0 term at a given angle γ, and b represents the first correction term at the same angle.

Although more than the first correction terms can be significant in Eqs. (22) and (23), the presence of the imaginary terms in Eq. (23) is a significant fact that should not be overlooked. The presence of the imaginary terms makes the power radiated into the side lobes less dependent on array orientation for an odd number of elements than for an even number. Thus, for nearly equal numbers of elements, an odd number of elements is to be preferred from the standpoint of reducing gain modulation due to array rotation.

d. OMNIAZIMUTH PATTERNS

For certain portions of a space mission, it is conceivable that it would be desirable to use the same array circuitry to form a pattern that was essentially uniform in the plane perpendicular to the spin axis of the space probe, rather than the usual retrodirective pattern. This brief section will point out the proper approach to forming an omniazimuth patpern, and will also warn against a poor approach.

The proper way to form an omniazimuthal pattern with a circular array is to feed all elements with equal current magnitude and with a progressive phase difference between adjacent elements such that there is an integer number of 2π radians phase change in going around the array. This technique was applied by Tillman, *et.al.*;[14] see also the references given in that paper. Out of the azimuth plane, the array factor provides directivity in addition to that provided by the elements in the array.

A second, but not recommended, way to approximate an omniazimuth pattern would be to feed all the elements with the same phase. The array factor for an infinite number of elements would then have a pattern given by[4]

$$E = J_0(2\pi R \sin\theta) \quad , \tag{31}$$

where θ is the angle measured from the array spin axis (perpendicular to the plane of the array). The peak of the array factor is along the array spin axis, but the array diameter in wavelengths could be chosen so that one of the side lobes was in the azimuth plane. The element pattern of the individual array elements could then be chosen, in principle, to suppress the main beam and other side lobes of the array factor. There are three problems with this approach. First of all, the positions of the side lobes of the array factor change with frequency, so that a small

change in operating frequency would scan the desired "side lobe" of Eq. (31) out of the azimuth plane. As an example, with an array about 20 wavelengths in diameter, a frequency change of only ±2.5 percent would place a null rather than a peak of the array pattern in the azimuth plane. Secondly, the element pattern would have to have very low response off of its peak in order to be effective in suppressing the main beam and other side lobes of the array factor. Thirdly, for a finite number of elements, correction terms have to be added to Eq. (31), which will produce ripple in the azimuth pattern of the array.[4] For a given number of array elements, the ripple would be greater if the elements are driven in phase rather than with the proper phase progression. This statement is based on examination of Eq. (18) of Ref. 14.

3. Cylindrical Retrodirective Array of Discrete Unidirectional Line Sources with Logical Element Switching

a. INTRODUCTION

Another configuration of cylindrical antenna, which is particularly significant because mutual coupling between its elemental radiators can be made very small in practice, is one in which a number of discrete unidirectional line source radiators are located around the exterior surface of the spacecraft. Figure 15 provides an end view of such a cylindrical array, showing particular elemental antenna patterns that are directed radially outward.

For maximum overall gain of such an array, one should consider the use of logical circuitry (or other means) to turn off power to those elements that are not contributing substantially to radiation in the desired direction. Because all elements on the back side of the cylinder are invisible and cannot contribute any field in the desired direction, they could be turned off. Furthermore, the directivity patterns of the elemental radiators would most likely provide significantly less gain in the desired direction as the angle from the radial approaches ±90 degrees, so maximum gain would occur if somewhat less than 180 degrees of the array were energized.

The primary objective of this analysis is to determine the optimum included angle of energization for a cylindrical array of such elements. For simplicity the particular elemental azimuthal pattern used for the computation is the simple cosine-squared function.

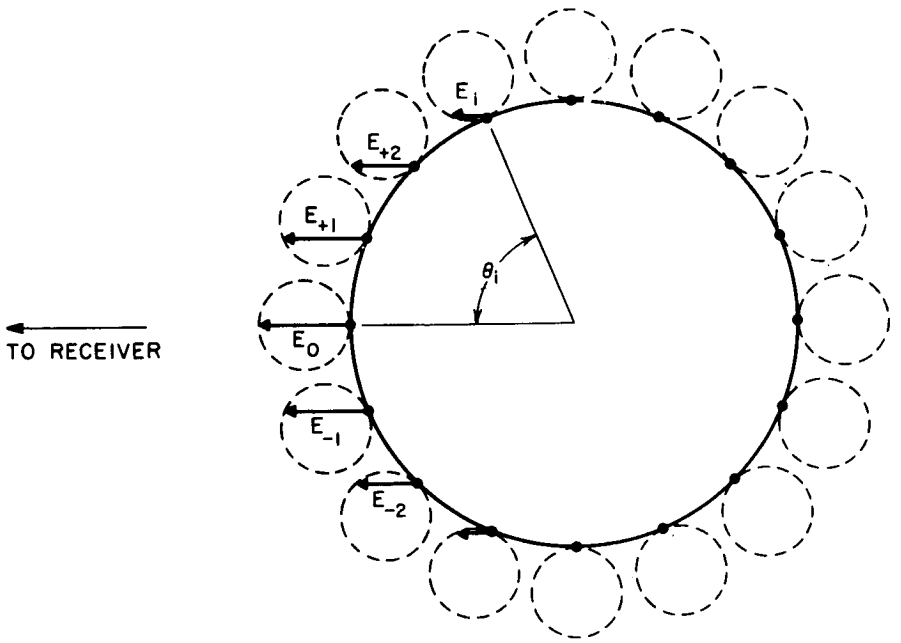

FOR A UNIDIRECTIONAL COS^2 POWER PATTERN:

$$E_i = \begin{cases} 2 \cos \theta_i, 0 \le |\theta_i| \le \pi/2 \\ 0, \pi/2 \le |\theta_i| \le \pi \end{cases}$$

TA-5574-30

FIG. 15 CYLINDRICAL ARRAY OF DISCRETE UNIDIRECTIONAL RADIATORS

b. ASSUMPTIONS

The following assumptions will be used for the analysis:

Array Configuration - A total of N^* elements are equispaced on the circumference of the cylinder. It is assumed that there is no interaction (mutual coupling) between the elements. Within the included angle of energization, each active element radiates unit power (which implies saturated amplifiers in the retrodirective circuitry) with the pattern described below.

Elemental Antennas - Each radiator is assumed to have a unidirectional cosine voltage pattern (*i.e.*, unidirectional cosine-squared power pattern) of the form

$$E_i = \begin{cases} 2 \cos \theta_i, & \text{for} \quad 0 \leq |\theta_i| \leq \pi/2 \\ 0, & \text{for} \quad \pi/2 < |\theta_i| \leq \pi \end{cases} , \tag{32}$$

where θ_i is the angle between the radial of the ith element and the radial to the distant receiver. It is to be noted that

$$\frac{1}{2\pi} \int_{-\pi}^{+\pi} (E_i)^2 d\theta_i = 1 ,$$

so all gains will be relative to omniazimuthal. All elements are polarized parallel to the cylinder axes. It is further assumed that adjacent elements are far enough apart to have negligible mutual coupling, so that the elemental pattern is constant and not a function of look angle.

Retrodirectivity - The array is phased by retrodirective techniques so that all the individual contributions are precisely in phase upon arrival at the distant receiving antenna; thus, the total field in the desired direction may be obtained by coherently summing the contributions of each active element.

* The symbols used for the discussion of a particular antenna type will in general be applicable only to that type.

b. SOLUTION

The parameters of interest are (a) RF power into the array, (b) effective radiated power (ERP) in the direction of the receiver, and consequently (c) the power gain, expressed as the ratio of (b) to (a), as a function of the included angle of energization, α.

i. Coordinate System

Let one element be located at $\theta = 0$, and call this the 0th element. Then, for equispaced elements,

$$\theta_i = \frac{2\pi i}{N}, \quad \text{where} \quad i = 0, \pm 1, \pm 2, \ldots \tag{33}$$

and N is the total number of elements on the cylinder. Thus the voltage contribution of the ith element can be expressed as

$$E_i = \begin{cases} 2 \cos\left(\frac{2\pi i}{N}\right), & \text{for} \quad 0 \leq |i| \leq \frac{N}{4} \\ 0, & \text{elsewhere} \end{cases} . \tag{34}$$

Now, consider an integer I describing the active elements, within an included angle α, as follows:

$$\theta_{max} = \frac{\alpha}{2} = \frac{2\pi I}{N} . \tag{35}$$

m From this it can be seen that

$$N_a = 2I + 1 = \text{No. of active elements.} \tag{36}$$

ii. Effective Radiated Power

The effective radiated power is proportional to the square of the sum of the voltage contributions of all active elements; thus,

$$\text{ERP} = E_T^2 = \left[\sum_{i=-I}^{+I} E_i\right]^2 \quad \text{in appropriate units.} \tag{37}$$

For $|\theta|_{max} \leq \pi/2$, $E_i = 2 \cos (2\pi i/N)$ so

$$\text{ERP} = \left[2 \sum_{i=-I}^{+I} \cos \left(\frac{2\pi i}{N} \right) \right]^2 \tag{38}$$

Using the fact that

$$\sum_{i=-m}^{+m} \cos ix = 1 + 2 \cos x + 2 \cos 2x + \ldots + 2 \cos mx$$

$$= \frac{\sin (m + 1/2)x}{\sin 1/2x} \quad , \tag{39}$$

we have for Eq. (38)

$$\text{ERP} = \frac{4 \sin^2 \left(\frac{2\pi I}{N} + \frac{\pi}{N} \right)}{\sin^2 \left(\frac{\pi}{N} \right)} \tag{40}$$

But,

$$\frac{2\pi I}{N} = \theta_{max} = \frac{\alpha}{2} \quad ,$$

so

$$\text{ERP}(\alpha) = 4 \cdot \frac{\sin^2 \left(\frac{\alpha}{2} + \frac{\pi}{N} \right)}{\sin^2 \left(\frac{\pi}{N} \right)} \quad , \quad \text{for } \alpha \leq \pi \quad . \tag{41}$$

If, however, $N >> \pi$ and $\alpha/2 >> \pi/N$, we can use the approximations

$$\sin^2 \left(\frac{\alpha}{2} + \frac{\pi}{N} \right) \approx \sin^2 \left(\frac{\alpha}{2} \right) \quad ,$$

and

$$\sin^2 (\pi/N) \approx \pi^2/N^2$$

Then, Eq. (41) becomes

$$\mathrm{ERP}(\alpha) \approx \frac{4}{\pi^2} \cdot N^2 \cdot \sin^2\left(\frac{\alpha}{2}\right) \tag{42}$$

iii. RF Power Input

With unit power in each active element,

$$P_{in} = N_a = 2I + 1 = \left(\frac{\alpha}{2\pi}\right) N + 1 \tag{43}$$

The above is an exact mathematical expression, but for $N >> \pi$

$$P_{in}(\alpha) \approx \left(\frac{\alpha}{2\pi}\right) N \tag{44}$$

iv. Power Gain

Using the exact expressions (41) and (43) for ERP and P_{in}, we have

$$G = \frac{\mathrm{ERP}}{P_{in}} = \frac{4 \sin^2 (\alpha/2 + \pi/N)/\sin^2 (\pi/N)}{(\alpha/2\pi)N + 1} \quad , \quad \text{for } \alpha \leq \pi \tag{45}$$

This again is an exact expression; using our simplifying assumptions it reduces to

$$G(\alpha) \approx \frac{4N}{\pi^2} \cdot \frac{\sin^2 (\alpha/2)}{(\alpha/2\pi)} \quad , \text{ for } \quad 0 \leq \alpha \leq \pi \quad . \tag{46}$$

Figure 16 displays ERP, P_{in}, and G as a function of the included angle α.

v. Angle of Energization for Maximum Gain

The simplified expression (46) for power gain is a transcendental function of α. A numerical solution was obtained for the maximum, at

$$\alpha = 133.57^\circ = 2.3312 \text{ radians} \quad . \tag{47}$$

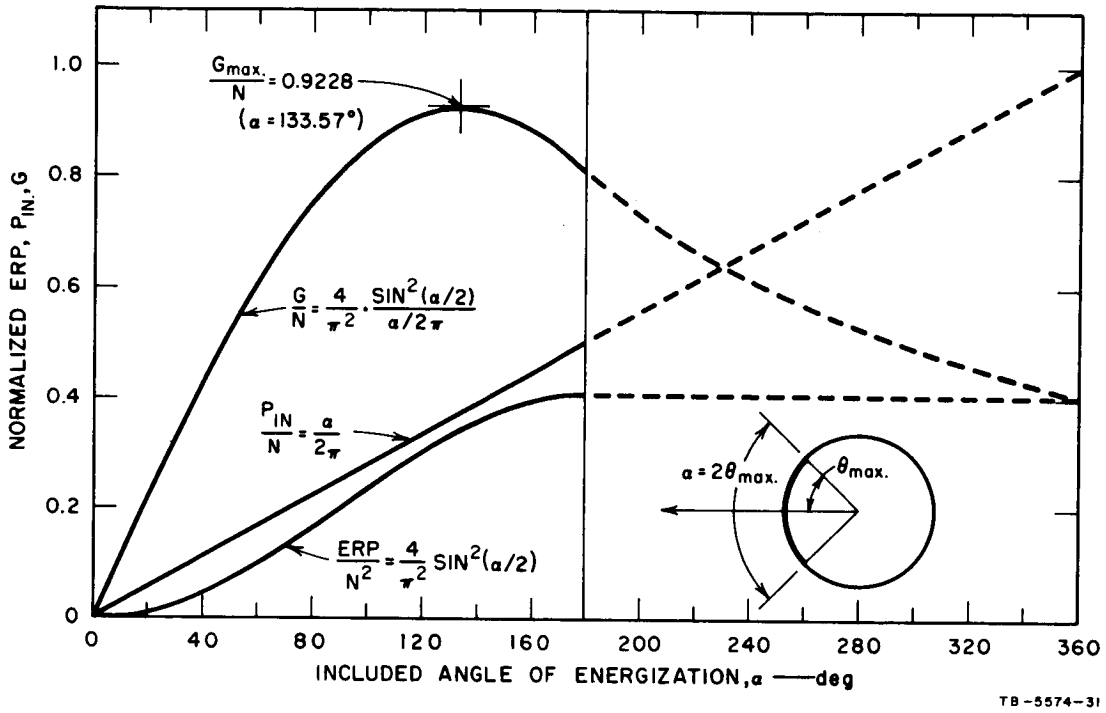

FIG. 16 NORMALIZED ERP, P_{in} AND G AS A FUNCTION OF α

At this optimum value of α,

from (42), ERP = 0.3434 N^2

from (44), P_{in} = 0.371 N

from (46), G = 0.9228 N

vi. Comparison of Different Angles of Energization

Table I below illustrates the gain (above omniazimuthal) of an "optimum" cylindrical array (α = 133.57°), a hemi-cylindrical array,

Table I

COMPARISON OF ARRAY GAINS

ANTENNA TYPE	GAIN (ABOVE OMNIAZIMUTHAL)	
	G	dB
Optimum Cylinder Array (α = 133.57°)	0.9228 N	10 log N - 0.35
Hemi-Cylinder Array (α = 180°)	0.8104 N	10 log N - 0.91
Full-Cylinder Array (α = 360°)	0.4052 N	10 log N - 3.92

and a full cylindrical array, where the active elements have a unidirectional cosine-squared power pattern.

From Table I it may be seen that, for a given number of elements on a cylinder, the gain of the hemi-cylindrical array is two times (3 dB) greater than the full cylindrical array, and that the optimum angle of energization (α = 133.57°) yields approximately 0.56 dB more gain than the hemi-cylindrical array, and an antenna whose gain is only 0.35 dB less than the postulated maximum possible value.

B. TASK II- ENVIRONMENTAL EFFECTS

1. General

Planetary reflections are important in any communication system when the space vehicle is within many thousands of miles and illuminates the planet. The effects of planetary reflections upon retrodirective array signal characteristics have been studied. A general description is presented here for the case when amplifier gain is linear at the retrodirective array subapertures. A more comprehensive report on the study will be included in the final report.

2. Planetary Model

Pulse measurements of backscattering from the moon at 3000 MHz indicate the moon is a rough surface and diffuse scatterer at that frequency.[15] The pulse shape and fluctuation can be explained by diffuse reflection rather than by specular reflection from several smooth areas on the moon's surface. Measurements at 400 MHz, however, indicate the radar echo from the moon is a combination of specular reflection from a quasi-smooth surface and diffuse reflection from a rough surface with the former predominating.[16-18] The power reflectivity of the moon for CW and long-pulse transmission (pulse length $\gtrsim$ 200 μs) lies between 0.1 and 0.01.[19] The reflectivity is reduced for short pulses which see a smaller cross-section than larger pulses. The power reflectivity corresponding to a pulse of 5 μs duration or shorter is typically 5×10^{-4}.

Venus is a better reflector than the moon with a power reflectivity of 0.10 to 0.15 (CW and long pulse transmission).[19] Radar measurements indicate that the roughness of Venus is comparable to the roughness of the moon.

Thus, planetary surfaces should have rms surface roughness dimensions in many wavelengths at frequencies considered for retrodirective arrays on space vehicles (frequencies $\gtrsim$ 1000 MHz). The power reflection coefficient of rough planetary surfaces should typically be less than 0.1.[19] Signals reflected from the surfaces will be diffuse and will statistically fluctuate in time due to the rotation of the planet and the movement of the space vehicle. The statistics of fading should in general be described by the Rayleigh distribution.

The fluctuations in the reflected signal from the planet will be correlated at all retrodirective array subapertures. As a result of this signal correlation, the retrodirective antenna, if it were only to handle signals reflected from the planet, would still produce a coherently summed signal at the distant (Earth) receiving station (assumed to be located at the pilot transmitting station). There would, however, be a superimposed phase and amplitude modulation, which would be a function of the surface roughness and the relative rotation of the planet and retrodirective link. When the direct link between the Earth station and the vehicle is also considered, the planetary reflected signal will not be correlated with the direct signal.

3. Received Signal Power

The signals received at retrodirective array subapertures interrogated by both direct and planetary reflected signals will be uncorrelated and will add in power. The received power at subapertures interrogated by only a planetary reflected signal will be a maximum of 10 percent of the power received by those apertures directly interrogated, assuming a 10 percent power reflectivity at the planetary surface.

Thus the signal power received at the terminal receiving antenna, assuming all subapertures under consideration are interrogated by both direct and planetary reflected signals, might fluctuate as much as 0.5 dB above the nominal level if no planet existed. If half of the subapertures are interrogated by direct signals and half by planetary reflected signals, *i.e.*, when the vehicle is near the line joining the planet and the terminal station, if the vehicle were near the planet, and if equal power output is directed at all activated subapertures, the power received could be 55 percent of the power received if no planet existed. Roughly 3 dB gain in power could be obtained by activating in the transmission mode only subapertures interrogated directly.

Activating only selected subapertures in the transmission mode would require a signal-to-noise sensing device that activates the transmitting circuit only above a minimum threshold. The minimum threshold could, for instance, be 10 or 20 percent of the maximum subaperture signal-to-noise ratio.

Planetary reflections can modify the "free-space" retrodirective antenna pattern. The power pattern can thus vary by 10 percent of the maximum level.

4. Spectral Broadening

Signals reflected from rough planetary surfaces will be spread in Doppler frequency. The characteristics of the Doppler spread is dependent upon surface roughness characteristics and upon relative motions of the transmitter, the receiver, and the planet. Doppler spread may determine the minimum input receiver bandwidth and thus the maximum received signal-to-noise ratio.

Doppler spread, if planetary rotation determines the relative motion of the planetary reflecting surfaces and the elementary scatterers, can be in order of tens of Hz for the Moon, Venus, and Mercury, thousands of Hz for Mars, Pluto, and Neptune, and hundreds of thousands of Hz for Jupiter and Uranus.[19] If the relative surface and scatterer motion is determined by spacecraft velocities (transmitter and/or receiver), the Doppler spread could be thousands of Hz.

C. TASK III—CIRCUITRY

1. Estimated Amplifications, and Noise Bandwidths for Retrodirective Elements on a Planetary Bus

a. INTRODUCTION

If a bus to Mars, say, is to employ a retrodirective array for transmission back to Earth, then the active circuitry of the bus must provide a very high power gain in order to satisfy mission requirements. A primary purpose of the following calculations is to determine (approximately):

(1) The required power amplification for each active retrodirective element, and

(2) The maximum allowable noise bandwidth for each element.

b. MARS MISSION PARAMETERS

For estimating purposes, we will take the following parameters from the Mariner IV flight:

d = 135×10^6 statute miles (at Mars encounter)

F_r = 2.1 GHz (spacecraft receive frequency)

F_t = 2.3 GHz (spacecraft transmit frequency)

T_e = 10^4 W (Earth transmitter carrier power) (70 dBm)

We shall also assume the new 210-ft diameter Goldstone antenna is used, which, if an illumination efficiency of 54 percent is assumed, provides the following gains:

G_t = + 60.3 dB (2.1 GHz)

G_r = + 61.1 dB (2.3 GHz)

And, we shall assume that the active bus transmitters (*i.e.*, retrodirective elements) will develop a total of 20 W of RF at 2.3 GHz.

A look ahead to Table II and Figs. 17-19 will also show the use of the following assumed parameters:

L_1 = Earth transmission circuit loss = 1.0 dB

L_2 Bus receiving circuit loss = 1.0 dB

L_3	= Bus transmitting circuit loss	=	1.0 dB
L_4	= Earth receiving circuit loss	=	1.0 dB
T_h	= Noise temperature of bus receivers	=	1450°K
C/N	= Required carrier-to-noise ratio in each retrodirective circuit of bus	=	+10.0 dB

c. RETRODIRECTIVE CYLINDRICAL ARRAY ANTENNA

All previous antenna configurations have been based on the assumption that spin stabilization will obviate the need for pointing the beam of a retrodirective antenna in the elevation plane. It has been generally assumed that the beam would always point somewhere in the plane perpendicular to the spin axis. In the following analysis the more general case of an antenna capable of pointing in nearly any direction (except near the zeniths) is assumed. In addition, the retrodirective cylindrical array on the bus is assumed to have a 10λ radius and 10λ axial dimension. Each element is an axial $\lambda/2$ dipole, spaced $\lambda/4$ above the conducting surface of the cylinder. Elements are spaced $\lambda/2$ along the axial dimension (yielding 20 elements/row) and are spaced $\lambda/2$ along the circumference (yielding $40\pi \approx 125$ elements/ring), for a total of 2500 elements on the cylinder.

It is further assumed that logic circuitry is employed to turn off those elements that are not substantially contributing to radiation in the desired direction; only those rows within an included angle of 144 degrees (50 rows) are assumed active and all available power is equally distributed among them (see Task 1, section 3 above), to give near optimum ERP; so there are $50 \times 20 = 1000$ active elements in the array.

For the $\lambda/2$ elemental dipoles described, the gain is approximately +4.4 dB (above isotropic) for the elements directly in line with the direction of the incoming wave ($\theta = 0$ degrees), and is approximately -2.0 dB for the extreme active elements ($\theta = \pm 72$ degrees). (The average gain of all active elemental dipoles can be shown to be approximately +3.3 dB the effect of mutual coupling between dipoles is neglected.)

d. CALCULATIONS

With the essential parameters now defined, we proceed with the calculations. For the given array, we shall consider three different bases (configurations) of elemental dipoles and receivers:

(1) One receiver per dipole (Fig. 17)
(2500 receivers required)

(2) One receiver per axial row of dipoles (Fig. 18)
(125 receivers required)

(3) One receiver per array (Fig. 19)
(1 receiver required)

The second configuration (one receiver per row) is probably the only one of practical interest, although inclusion of the other two provides useful references for comparison.

Table II gives the results of the calculations, and Figs. 17-19 display the levels, gains and attenuations in block diagram form.

Required Amplification—Reference to Table II shows that each active retrodirective unit must be capable of the order of 150 dB power amplification of the received pilot, in order to produce the required output level. Note that the required amplification per retrodirective unit is the same for all three illustrated configurations. The point is, that for assumptions of (1) fixed total antenna aperture size, and (2) fixed total RF power in and out of the total aperture, then the required gain per subaperture is independent of the number of subapertures into which the total aperture is subdivided.

Noise Bandwidth—The maximum allowable noise bandwidth of each retrodirective unit does depend upon the subaperture size (how many elemental antennas per receiver), and upon the minimum tolerable S/N in the retrodirective units. If we arbitrarily say that the average S/N shall be +10 dB, then reference to Table II shows that the second scheme (one receiver per row) has a maximum allowable noise bandwidth of approximately 4280 Hz.

e. CONCLUSIONS

It has been shown that each active retrodirective unit on a Mars bus must be capable of approximately 150 dB power amplification of the received pilot, and that for one receiver per row the maximum allowable noise bandwidth is approximately 4 Hz.

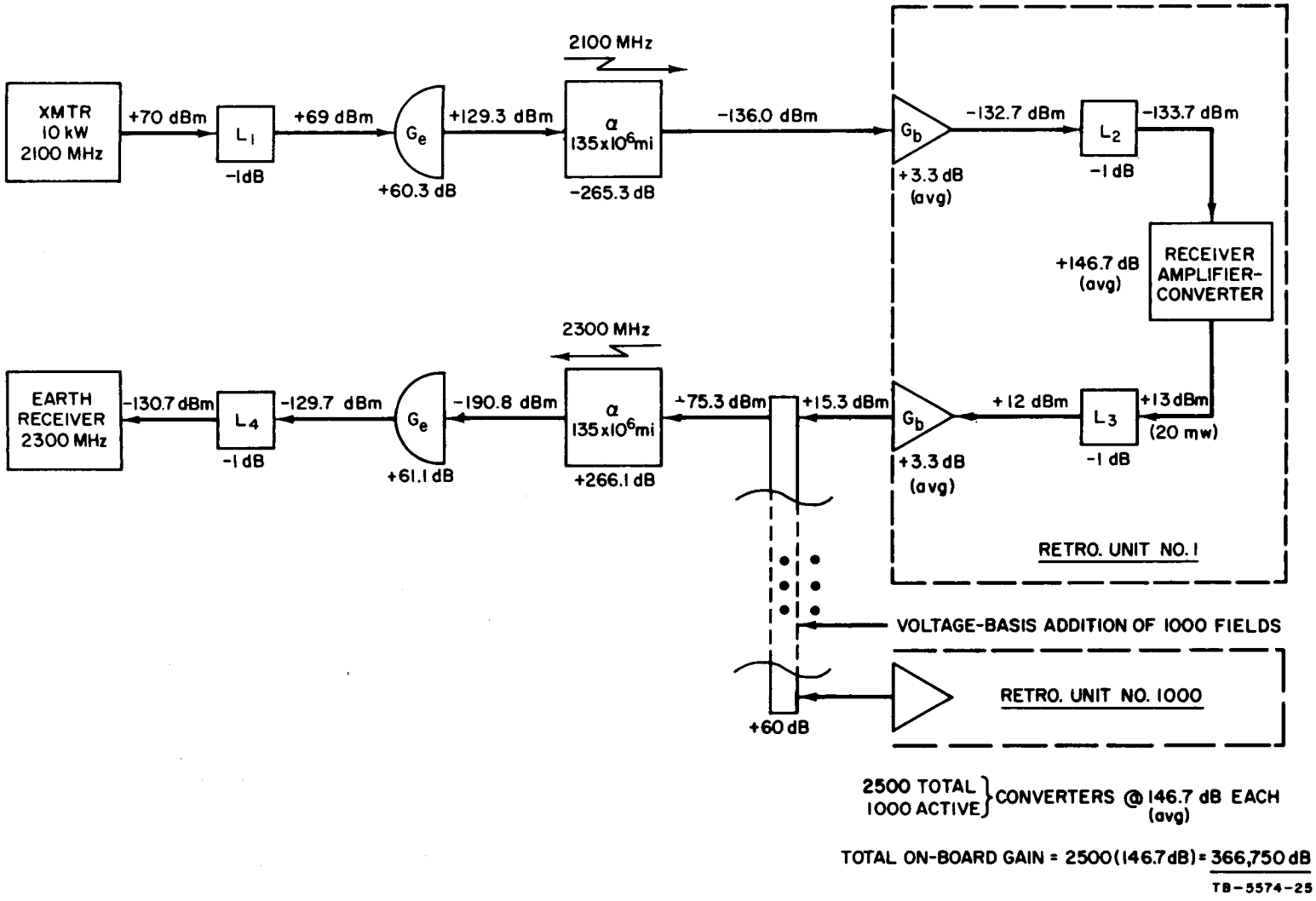

FIG. 17 EARTH/BUS LINK WITH 1000 ACTIVE CONVERTERS (One per active element)

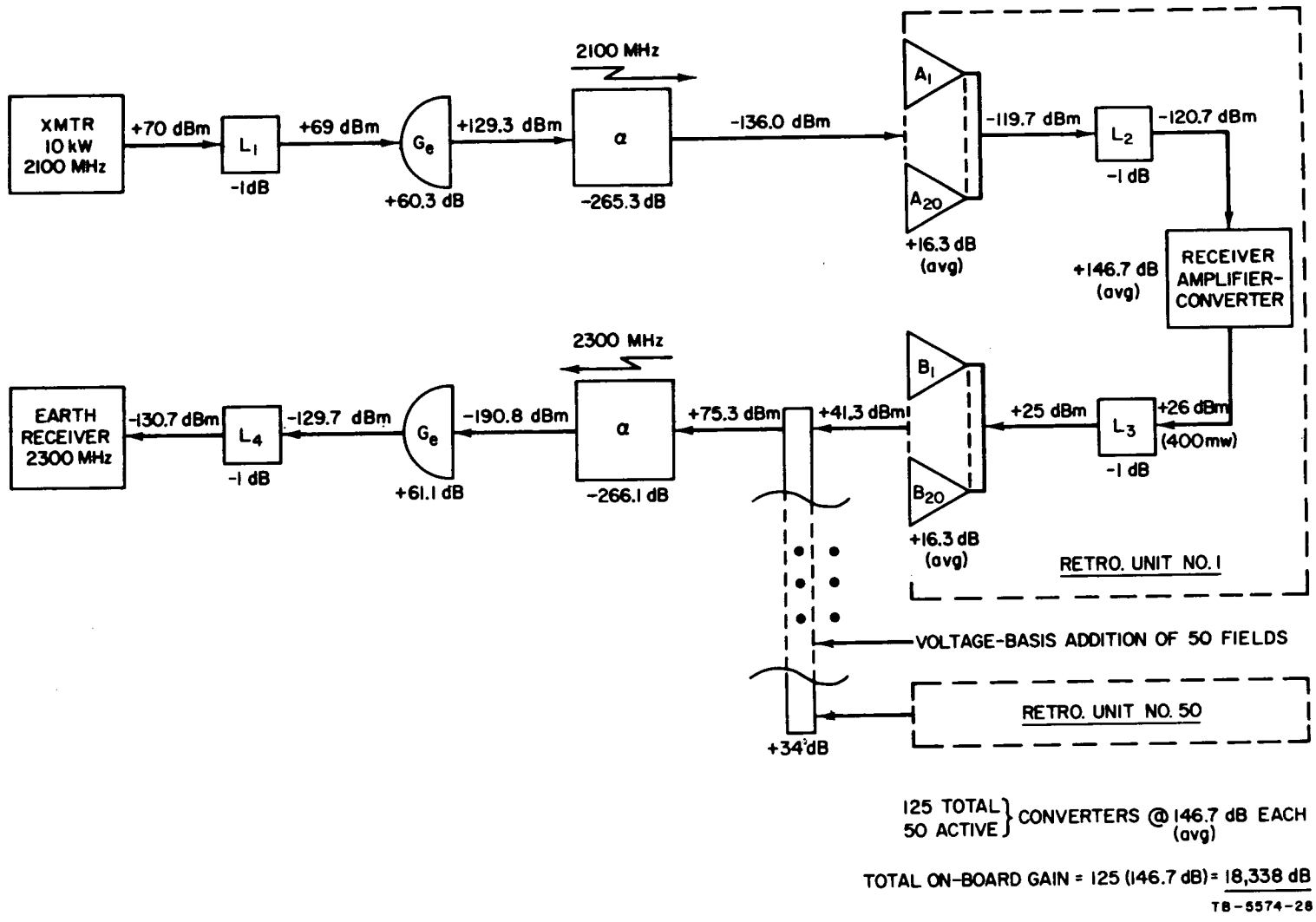

FIG. 18 EARTH/BUS LINK WITH 50 ACTIVE CONVERTERS (One per active row)

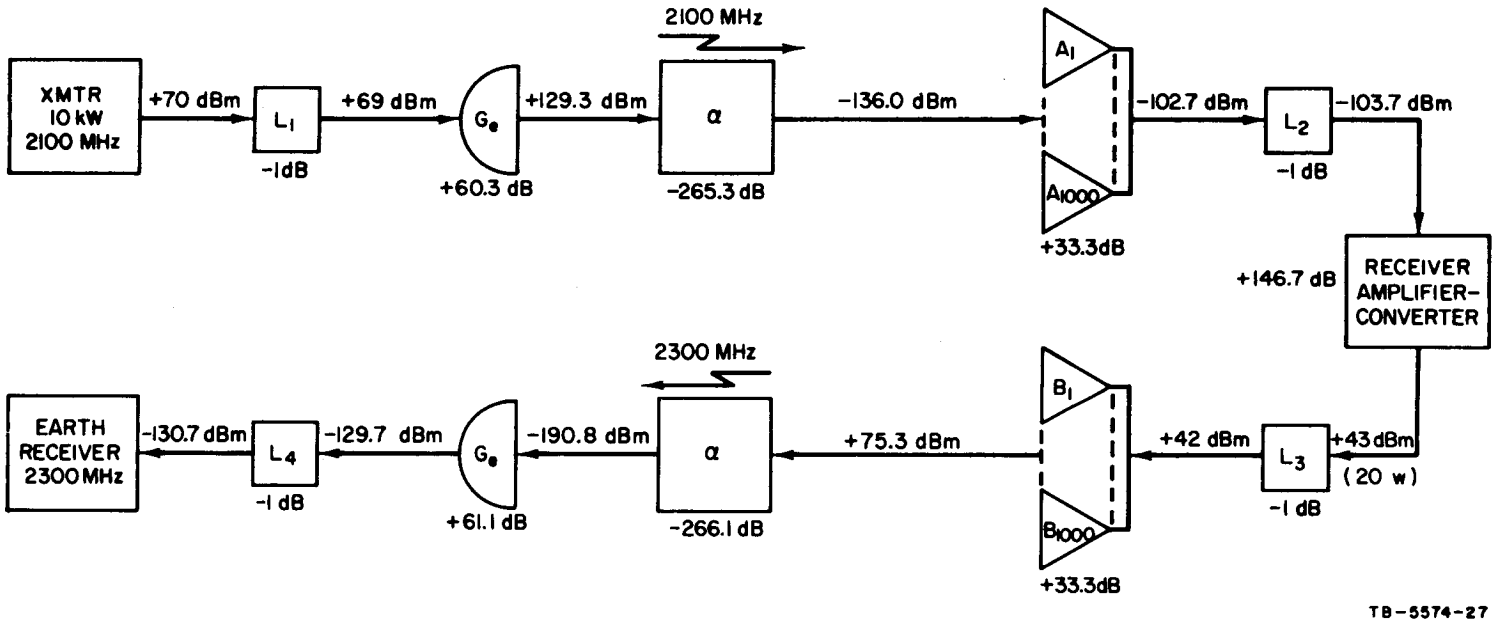

FIG. 19 EARTH/BUS LINK WITH ONE ACTIVE CONVERTER

Table II

EARTH/BUS LINK WITH VARIOUS RECEIVER BASES

PARAMETER		RECEIVER BASIS		
		ONE/ELEMENT	ONE/ROW	ONE/ARRAY
T_e = Earth transmitter carrier power (10 kW)		+70.0 dBm	→	→
L_1 = Transmission circuit loss		-1.0 dB	→	→
G_e = Earth antenna gain (210 ft dia 54 percent eff)		+60.3 dB	→	→
α = Free-space attenuation (135 x 10^6 miles		-265.3 dB	→	→
G_b = Bus antenna gain per receiver ($\lambda/2$ axial dipoles, spaced $\lambda/4$ above cyl. surface)	Max: $\theta = 0°$	+4.4 dB	+17.4 dB	
	Avg:	+3.3 dB	+16.3 dB	+33.3 dB
	Min: $\theta = 72°$	-2.0 dB	+11.0 dB	
L_2 = Receiving circuit loss		-1.0 dB	→	→
C = Received carrier power	Max:	-132.6 dB	-119.6 dBm	
	Avg:	-133.7 dBm	-120.7 dBm	-103.7 dBm
	Min:	-139.0 dBm	-126.0 dBm	
W = Max. allowable noise bandwidth (T_n = 1450°K, C/N = +10 dB)	Max:	275 Hz	5500 Hz	
	Avg:	214 Hz	4280 Hz	214 kHz
	Min:	63 Hz	1260 Hz	
P_o = Required receiver-amplifier output level (for 20 W total)		+13 dBm (20 mW)	+26 dBm (400 mW)	+43 dBm (20 W)
G_a = Required receiver amplification	Min:	145.6 dB	→	
	Avg:	146.7 dB	→	→
	Max:	152.0 dB	→	
N = No. of receivers required		2500	125	1
G_T = Total on-board gain required = $N \cdot G_a$ (Avg.)		366,750 dB	18,338 dB	146.7 dB

The circuitry for retrodirective units of this performance will be quite complex, compared to the retrodirective circuitry which has appeared in the literature *t* for earth satellite application, where gains of less than 40 dB are specified and much wider bandwidths are employed.

With this high gain requirement, one important problem will be transmitter-receiver isolation.

A critical parameter in any retrodirective array is the phase stability and uniformity of the circuitry. It may be expected that, for conversion from 2.1 to 2.3 GHz with 150 dB power gain and 4 kHz noise bandwidth, phase stability and uniformity on the order of ± 10 degrees[2] will be a significant problem.

2. A Duplex Retrodirective Scheme for a Mars Bus

a. Requirements for a retrodirective scheme

It has been shown in Part C-1 above that each retrodirective transmitting unit on a Mars bus will require on the order of 150 dB of power amplification of the received pilot, and that the allowable noise bandwidth in each retrodirective unit is quite narrow (approx. 4000 Hz for a "row" antenna of 20 elements).

In addition, there are several other design constraints on a retrodirective scheme, for example:

(1) The scheme should permit precise determination of bus range rate (Doppler shift) at the earth station.

(2) Duplex operation will be required, which means, since both signals are CW, that there must be a frequency offset between receive (pilot) and transmit frequencies, and a relatively large separation (several percent) will ease filter requirements.

(3) Phase taper of the transmitted wave over the cylinder due to frequency offset should be negligible ($\ll \pi/2$) to realize maximum gain. This implies some form of compensation, if a substantial frequency offset is employed.

b. BASIC OPERATION OF THE SCHEME

The basic operation of the scheme presented here is that, by coherent division and multiplication, the retrodirective array transmits a frequency that is 9/8 of the received (pilot) frequency.* The scheme can use the carrier of the earth-bus command link as the retrodirective pilot; a separate pilot frequency is not required.

i. Master Receiver

First, an omniazimuthal receiving antenna located on the spin axis (see Fig. 20) provides one master phase-lock receiver with the basic Earth carrier (pilot) frequency, shift by the one way Doppler but free from any spectral splitting (phase modulation) caused by spin.

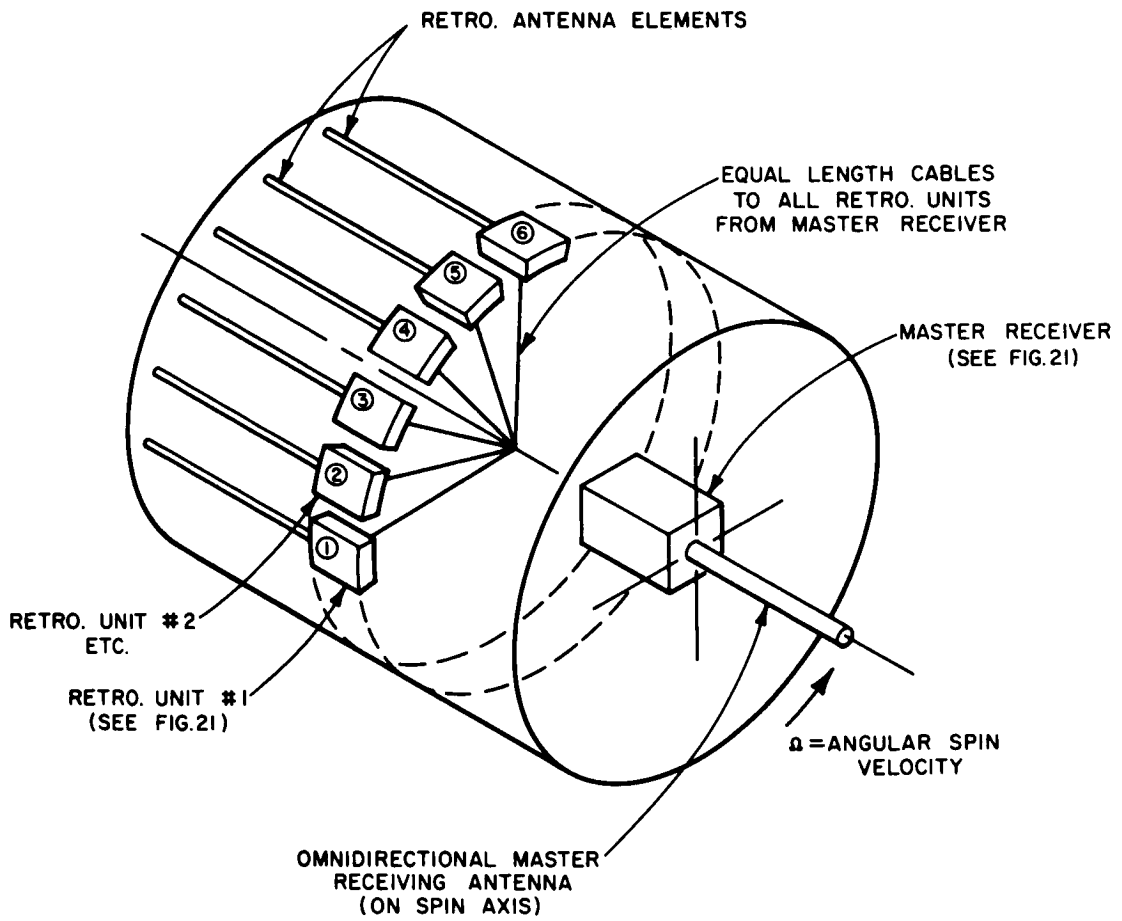

FIG. 20 PHYSICAL LAYOUT OF RETRODIRECTIVE ARRAY ON CYLINDRICAL LENS

* Any other convenient ratio of integers could be used.

This master receiver should be continuously phase-locked to the received carrier, except during transfer from one earth station to the next, as the on-axis antenna is always visible to the earth. Also, this master receiver is used as the command receiver. This scheme requires that the signal-to-noise ratio at this low-gain omniazimuthal antenna be greater than unity.

ii. Retrodirective Units

Each retrodirective unit contains a phase-lock loop, and the general functions of each retro unit (see Fig. 21) are:

(1) *Frequency Offset*—the pilot frequency is multiplied by 9/8 before amplification and retransmission.

(2) *Retrodirectivity*—each retro unit multiplies the spatial phase (relative to the plane of the incoming pilot wave) by 9/8, and conjugates, so the composite outgoing wave (at 9/8 F_r) is also planar and is radiated back in the direction from which the pilot signal (F_r) was received. Multiplication of the *spatial phase* by the same factor as the *frequency* (*e.g.*, 9/8) eliminates all phase taper.

(3) *Data Modulation*—the retransmission from each retro unit is phase modulated with spacecraft data and/or ranging modulation received from the Earth.

iii. Features of the Scheme

The following features of this retrodirective scheme may be compared with a simple "conventional" heterodyne approach:

(1) First mixer does not conjugate spatial phase as in the image frequency converter, for instance, because the injection frequency is *below* the receive frequency.

(2) Receive leg employs an IF of 1/25 F_r*, permitting amplification at a relatively low frequency.

* Any other convenient ratio of integers could be used.

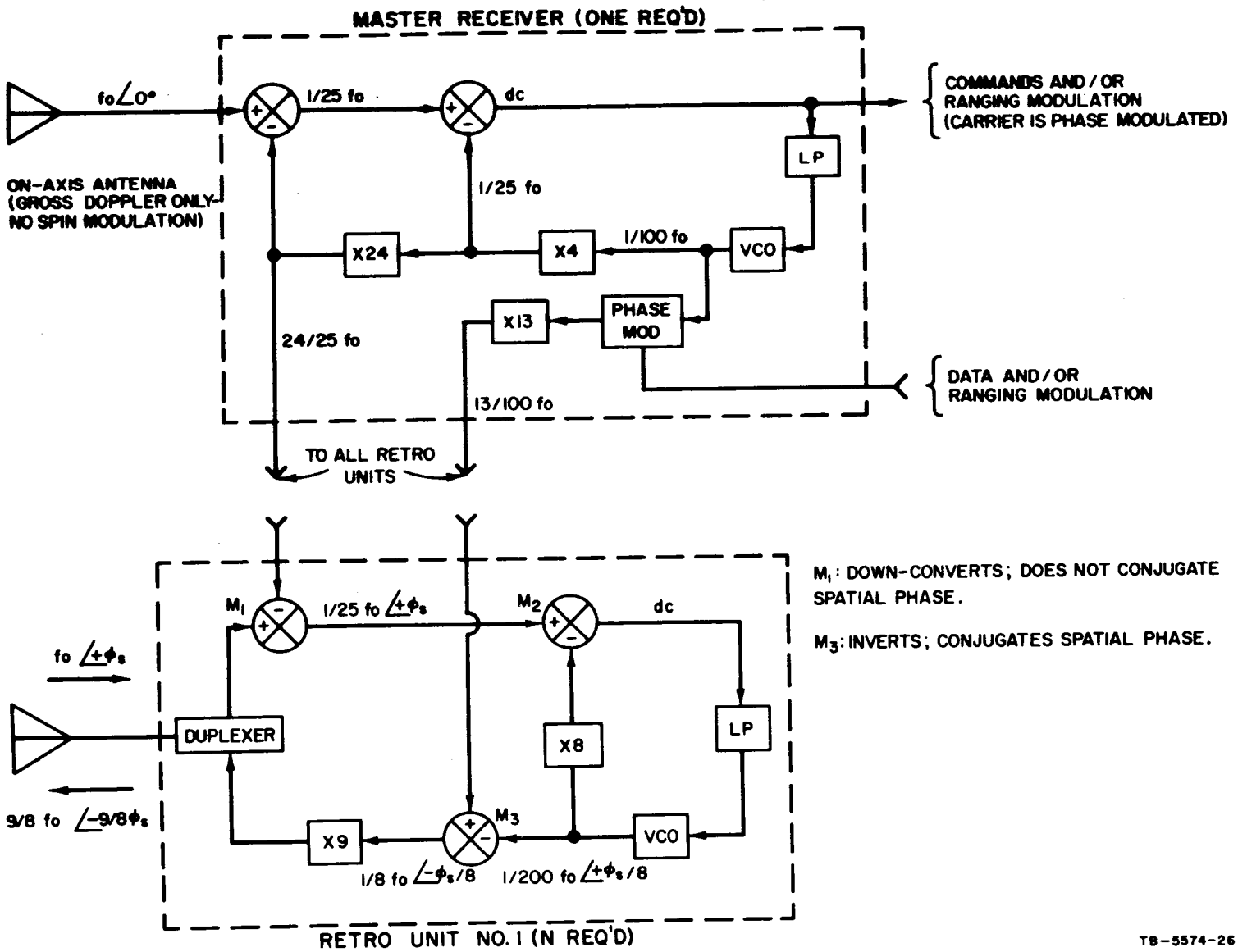

FIG. 21 CONVERSION SCHEME FOR A DUPLEX RETRODIRECTIVE SYSTEM

(3) Phase-lock loop employed in retro units to extract pilot, permits

(a) very narrow noise bandwidth, and

(b) potential for extracting phase-lock information for logical applications (*e.g.*, to control transmit leg, to determine attitude, and to sense malfunctions).

(4) Multipliers rather than RF amplifiers can be used in transmit legs.

c. GROSS DOPPLER SHIFT

Considering only Doppler shifts due to gross velocity of the bus, and assuming that the velocity does not change in one round-trip time, the bus receives a frequency which is precisely (relativistic)

$$F_r = \sqrt{\frac{1 - V/c}{1 + V/c}}\, f_{eB} \quad ,$$

where

f_{eB} = Earth transmit frequency

Gross velocity of bus c.g.

Our retrodirective scheme retransmits a signal of frequency

$$F_t = (9/8)F_r \quad ,$$

and applying the (relativistic) down-link Doppler, the earth receiver sees a frequency

$$F_e = \sqrt{\frac{1 - V/c}{1 + V/c}}\, F_t \quad ,$$

which yields

$$F_e = \left(\frac{1 - V/c}{1 + V/c}\right) \frac{9}{8} F_0$$

This is *precisely* equal to the two-way (radar) Doppler shift of a signal whose frequency is $(9/8)F_0$.

d. CONCLUSIONS

A method has been presented, by means of coherent division and multiplication, to obtain a relatively wide spacing between the receive (pilot) and transmit frequencies of a retrodirective cylindrical array. This method would be applicable to a scheme where duplexers were used on elemental antennas, or where separate transmit and receive antennas were used but associated antennas are on the same axial line of the surface of the cylinder.

Phase-lock loops are employed for the division function. If the low-pass filter in the loop passes only the modulation frequency, which is the same as the spin (1 Hz or less), any modulation of higher frequency will not pass through the retrodirective unit. Thus the carrier of the earth bus command link could also be used as the pilot for the retrodirective array, without having the command modulation appearing on the down-link signal, as long as the spectrum of the command modulation has no components in the passband (dc to 1 c/s) of the phase-lock loops.

Frequency multiplication is employed in the output of the retrodirective unit, so transistor and/or varactor multipliers would be a convenient way of producing power at approximately 2 GHz with good dc-to-RF conversion efficiency.

By using a signal derived from an antenna on the spin axis for the local oscillator, the scheme permits precise determination of bus range rate (Doppler shift) at the earth station. (It would perhaps be feasible to derive this signal by means of a summation of the signals from all retrodirective units, but the antenna on the spin axis is in any event conceptually useful.)

3. RANGE AND RANGE-RATE TRACKING

a. PHILOSOPHY

Both range and range-rate tracking involve phase (or frequency) comparison of a transmitted signal with the same signal reflected or transponded by the spacecraft being tracked. If the spacecraft transponder is other than an RF amplifier, a local oscillator is required in the spacecraft. Such an oscillator may be phase-locked to the received signal and hence has a frequency derived from and coherent with the

received frequency, as in the scheme presented in the above section. Relatively complex circuitry is required and signal acquisition may be a problem. Alternatively, the local oscillator may be free-running and the signal returned by the spacecraft must be designed so that the oscillator-frequency as well as range and range-rate information can be extracted by the tracking station.

The Goddard Space Flight Center system[20] is based on the second concept. The returned signal consists of a carrier and a modulated subcarrier; both the carrier frequency and the subcarrier frequency relative to that of the carrier are linear functions of the local oscillator frequency and of the Doppler offset.

b. RANGE-RATE TRACKING

For nonrelativistic radial velocities, the shift in frequency is directly proportional to the radial velocity. In the two-way systems considered here it is assumed that the velocity can be considered constant over the round-trip propagation time. Otherwise, more complex systems are needed or the measured Doppler can be considered as an average over the propagation time. Typically, the measurement is considered to be the vehicle radial velocity at the instant one-way propagation time in the past.

Range-rate systems require that the frequencies transmitted and those received be measured. The velocity is then easily calculated.

c. RANGE TRACKING

If a range-rate system can be kept in continuous operation starting from a known range, range can obviously be obtained from a simple integration of velocity. More typically, continuous operation is not obtained due to equipment malfunction and earth rotation and so cannot be relied upon. Then range must be determined separately.

Periodic ranging signals are frequently used. They should have three distinct properties:

(1) Minimum range uncertainty.

(2) No range ambiguity.

(3) Indication of needed correction.

The range uncertainty depends upon the width of the autocorrelation function peaks, which should be small. When tones are used, a high-frequency is required; with pulses, narrow widths are needed.

The range ambiguity depends upon the spacing of the periodic peaks of the autocorrelation function. Thus the period should exceed the round-trip propagation time for the maximum range of interest. With tones, a low frequency is required; with pseudorandom pulse sequences, a long period is required. Frequently, the ambiguity problem becomes much less severe because the approximate range is already known.

When, as is typically done, a copy of the transmitted signal is delayed and cross-correlated with the returned signal, the correlator output should indicate the change in delay required to achieve coincidence of the two signals. Tones have this property; pulse sequences do not. However, a pulse sequence derived from several shorter sequences can be used to simplify this search problem.

d. GODDARD SYSTEM

The Goddard system uses a free-running transponder oscillator. The up-signal is modulated with tones and/or pseudorandom codes. The signal received by the spacecraft is doubly converted to produce a subcarrier, which modulates a down-carrier derived from the same oscillator. Cascade phase-locked loops in the earth receiver extract Doppler and, incidentally, the transponder oscillator frequency. The transponder can receive up to three modulated signals simultaneously and convert the modulation to separate subcarriers.

e. EXTENSION OF GODDARD SYSTEM

For a configuration consisting of an earth station, a spacecraft bus, and a capsule, the returned signal must be designed so that the following can be extracted:

(1) Bus local oscillator frequency

(2) Capsule local oscillator frequency

(3) Earth bus Doppler

(4) Bus capsule Doppler.

A feasible configuration using one unmodulated and two modulated subcarriers is presented in Appendix A. This configuration has yet to be considered in relation to a retrodirective array or any other type of adaptive antenna.

f. CONCLUSIONS

Except for the fact that many amplifier/transmitters are required on a retrodirective array, only minor modifications of the basic Goddard transponder are required to derive Doppler for the earth/bus and the bus/capsule links. The resulting signals, when suitable ranging modulation is used, also can be processed to yield earth/bus and earth/bus/capsule range information.

No phase-locked circuits are required on either the bus or the capsule and only readily achievable oscillator stabilities are required in the vehicles.

4. MAXIMUM LIKELIHOOD ANGLE ESTIMATION FROM A UNIFORMLY SPACED n-ELEMENT LINEAR ARRAY

Consider an array of n elements separated by S wavelengths along a line and receiving a plane wave at an angle β from the perpendicular to the line of the array. Let

$$k = 2\pi S \sin \beta \tag{48}$$

and note that

$$|k| \leq 2\pi S \quad . \tag{49}$$

Let ϕ_i be the phase of the ith signal with respect to an arbitrary reference phase. Let a be the phase of the wave with respect to the reference at the first element. Then

$$\phi_i = a + k(i - 1) + n_i \quad , \tag{50}$$

where n_i is the phase noise of the ith measurement; in vector form:

$$\phi = aB + kA + N \quad , \tag{51}$$

where $b_i = 1$ and $a_i = i - 1$.

Consider the plane defined by the vectors A and B^* and consider unit vectors in that plane along B and perpendicular to B, U_1 and U_2 respectively.

Then

$$U_1 = \frac{B}{(B^T B)^{1/2}} \tag{52}$$

$$C = A - (A^T U_1) U_1 \tag{53}$$

$$U_2 = \frac{C}{(C^T C)^{1/2}} \tag{54}$$

Consider the additional unit vectors of an orthogonal basis,† all perpendicular to the plane, and the n-by-n transformation M

$$M = \begin{bmatrix} U_1^T \\ U_2^T \\ U_3^T \\ \hline U_n^T \end{bmatrix} . \tag{55}$$

Let

$$X = M\phi \tag{56}$$

$$Z = MN \tag{57}$$

and note that

$$B^T B = n$$

$$U_1 = \frac{B}{n} \tag{58}$$

---

* The transpose of B is denoted by B^T

† See Appendix B.

$$C = A - \left[\frac{n(n-1)}{2} \cdot \frac{1}{\sqrt{n}}\right] \frac{B}{\sqrt{n}}$$

or

$$C_i = (i-1) - \frac{n-1}{2} = \left(i - \frac{n+1}{2}\right)$$

$$C^T C = \sum_{i=1}^{n} \left(i - \frac{n+1}{2}\right)^2$$

$$= \sum_{i=1}^{n} \left[i^2 - (n+1)i + \frac{(n+1)^2}{4}\right]$$

$$= \frac{n(n+1)(2n+1)}{6} - (n+1)\frac{n(n+1)}{2} + \frac{(n+1)(n+1)n}{4}$$

$$= \frac{n(n+1)}{12}[4n + 2 - 3n - 3] = \frac{(n+1)n(n-1)}{12} \qquad (59)$$

and therefore

$$X_1 = U_1^T \phi = \frac{1}{\sqrt{n}} \sum_{i=1}^{n} \phi_i$$

$$= aU_1^T B + kU_1^T A + U_1^T N$$

$$= a\sqrt{n} + k\sqrt{n}\,\frac{n-1}{2} + \frac{1}{\sqrt{n}} \sum_{i=1}^{n} n_i \qquad (60)$$

and

$$X_2 = U_2^T \phi = \left[\frac{12}{(n+1)n(n-1)}\right]^{1/2} \sum_{i=1}^{n} \left(i - \frac{n+1}{2}\right)\phi_i \qquad (61)$$

also

$$X_2 = U_2^T (aB + kA + N)$$

but

$$U_2^T B = nU_2^T U_1 = 0 \tag{62}$$

and

$$U_2^T A = \frac{[A - (A^T U_1)U_1]^T}{(C^T C)^{1/2}} \cdot A = \frac{A^T A - (A^T U_1)^2}{(C^T C)^{1/2}}$$

$$= \left[\frac{n(n-1)(2n-1)}{6} - \frac{n(n-1)^2}{4}\right]\left[\frac{12}{n(n+1)(n-1)}\right]^{1/2}$$

$$= \left[\frac{n(n-1)(4n-2-3n+3)}{12}\right]\left[\frac{12}{n(n+1)(n-1)}\right]^{1/2} = \left[\frac{n(n+1)(n-1)}{12}\right]^{1/2} . \tag{63}$$

Hence

$$X_2 = k\left[\frac{n(n+1)(n-1)}{12}\right]^{1/2} + \left[\frac{12}{(n+1)n(n-1)}\right]^{1/2} \sum_{i=1}^{n} \left(i - \frac{n+1}{2}\right) n_i \quad . \tag{64}$$

Further, $X_3 \ldots . X_n$ are, of course, functions of ϕ

$$X_j = U_j^T \phi \tag{65}$$

but, using (51), and noting that

$$U_j^T B = U_j^T A = 0 \tag{66}$$

for

$$j \geq 3$$

such

$$X_j = U_j^T N \tag{67}$$

and are not functions of a or k.

If we assume that the n_i are independent normal variables with zero means and variances σ^2, the maximum likelihood estimates of a and k will be those values, $\hat{a}$ and $\hat{k}$, $|\hat{k}| \leq 1$ such that the probability density

$$p(n) = (2\pi\sigma^2)^{-\frac{n}{2}} \exp -\frac{1}{2\sigma^2} N^T N \tag{68}$$

is maximized or equivalently $N^T N$ is minimized.

From (56) and (51)

$$X = M\phi = aMB + kMA + Z \tag{69}$$

or

$$X_1 = a\sqrt{n} + k\sqrt{n}\,\frac{n-1}{2} + \frac{1}{\sqrt{n}} \sum_{i=1}^{n} n_i \tag{70a}$$

$$X_2 = \left[\frac{n(n+1)(n-1)}{12}\right]^{1/2} + \left[\frac{12}{(n+1)n(n-1)}\right]^{1/2} \sum_{n=1}^{n} \left(i - \frac{n+1}{2}\right) n_i \tag{70b}$$

$$X_j = U_j^T N = Z_j \quad j = 3, 4, \ldots n \tag{70c}$$

The covariance matrix for the Z's

is

$$T = E(ZZ^T) = E(MNN^T M^T)$$

$$= ME(NN^T)M^T \quad .$$

$$= \sigma^2 MM^T = \sigma^2 \tag{71}$$

and the probability density for the Z's is

$$f(Z/a,k) = (2\pi\sigma^2)^{-\frac{n}{2}} \exp$$

$$-\frac{1}{2\sigma^2}\left[\left(X_1 - \sqrt{na} - \sqrt{nk}\frac{n-1}{2}\right)^2 + \left\{X_2 - \left[\frac{(n+1)n(n-1)}{12}\right]^{1/2} k\right\}^2\right.$$

$$\left. + \sum_{i=3}^{n} X_i^2\right] \tag{72}$$

We can maximize this probability, regardless of k, by picking a so that the first term vanishes and by taking $\hat{k} = d$

where

$$d = \left[\frac{12}{(n+1)n(n-1)}\right]^{1/2} X_2$$

$$= \left[\frac{12}{(n+1)n(n-1)}\right] \sum_{i=1}^{n} \left(i - \frac{n+1}{2}\right) \phi_i \tag{73}$$

if $|d| < 2\pi S$, otherwise $\hat{k} = SGN(d) \cdot 2\pi S$ where $SGN(d)$ is the sign of d.

Consider those case with $|d| \leq 2\pi/S$.

Then

$$k = \frac{1}{(C^TC)^{1/2}} \cdot X_2 = \frac{1}{(C^TC)^{1/2}} U_2^T \phi$$

$$= \frac{1}{(C^TC)^{1/2}} U_2^T [aB + kA + N] \tag{74}$$

But

$$U_2^T B = 0 \tag{62}$$

and

$$U_2^T A = (C^T C)^{1/2} \tag{63}$$

$$\therefore \hat{k} = k + \frac{U_2^T}{(C^T C)^{1/2}} N \tag{75}$$

and the estimation error is

$$\hat{k} - k = \frac{C^T}{C^T C} N \quad . \tag{76}$$

The estimate is unbiased:

$$E(\hat{k} - k) = \frac{C^T}{C^T C} E(N) = 0 \tag{77}$$

and the variance is

$$\sigma_k^2 = E(\hat{k} - k)^2 = E\left(\frac{N^T C}{C^T C}\right)^T \left(\frac{N^T C}{C^T C}\right)$$

$$= E\frac{C^T}{C^T C} \cdot N N^T \frac{C}{C^T C}$$

$$= \frac{C^T}{C^T C} E(NN^T) \frac{C}{C^T C}$$

$$= \sigma^2 \frac{C^T I C}{C^T C C^T C} = \frac{\sigma^2}{C^T C}$$

$$= \frac{12}{(n+1)n(n-1)} \sigma^2 \quad . \tag{78}$$

For large n

$$\sigma_k^2 \simeq \frac{12\sigma^2}{n^3}$$

or

$$\sigma_k \simeq \frac{\sqrt{12}\sigma}{n^{3/2}} \tag{79}$$

If $\sigma = \pi/4$, then for various values of n

Table III

n	$c^T c$	$\sqrt{c^T c}$	σ_k (radians)
3	2	1.41	0.557
4	5	2.23	0.353
5	10	3.16	0.249
6	17.5	4.18	0.188
7	28	5.29	0.149
8	42	6.48	0.121

The remaining residual is

$$R(\phi) = U[|d| - 2\pi S]\left\{|X_2| - \left[\frac{(n+1)n(n-1)}{12}\right]^{1/2} 2\pi S\right\}^2 + \sum_{i=3}^{n} X_i^2 \tag{80}$$

Since phase detectors can normally read unambiguously only in a 2π range, say

$$-\pi < \phi_i < \pi \quad , \tag{81}$$

the set of data ϕ may have arisen from any of 3^n actual conditions where the observed phase in ϕ_i and the true phase is ϕ_i' and

$$\phi_i' = \phi_i \tag{82a}$$

or

$$\phi_i' = \phi_i + 2\pi \tag{82b}$$

or

$$\phi_i' = \phi_i - 2\pi \tag{82c}$$

Therefore $R(\phi)$ should be computed for each possible ϕ' and that data set which minimizes $R(\phi)$ should be used.

It is actually possible to divide the data space into regions and to associate with each region a translation vector to give the ϕ' which yields a minimum $R(\phi)$ and hence a maximum likelihood estimate of k. As an example, division of the data space for the case of $n = 3$ is treated below. In this case, using the above notation

$$U_1 = \begin{bmatrix} 1/\sqrt{3} \\ 1/\sqrt{3} \\ 1/\sqrt{3} \end{bmatrix} \quad U_2 = \begin{bmatrix} -1/\sqrt{2} \\ 0 \\ 1/\sqrt{2} \end{bmatrix} \text{ and } U_3 = \begin{bmatrix} 1/\sqrt{6} \\ -2/\sqrt{6} \\ 1/\sqrt{6} \end{bmatrix} . \tag{83}$$

Thus

$$M = \frac{1}{\sqrt{6}} \begin{bmatrix} \sqrt{2} & \sqrt{2} & \sqrt{2} \\ -\sqrt{3} & 0 & \sqrt{3} \\ 1 & -2 & 1 \end{bmatrix} \tag{84}$$

Thus the residual is

$$R = X_3^2 + [|X_2| - \Gamma 2\pi]^2 U[|X_2| - \sqrt{2}\pi] \tag{85}$$

where

$$X_2 = \frac{1}{\sqrt{2}}[- \phi_1 + \phi_3] \tag{86a}$$

$$X_3 = \frac{1}{\sqrt{6}}[\phi_1 - 2\phi_2 + \phi_3] \tag{86b}$$

Since the ϕ's are only measured within the interval $-\pi$ to π, then

$$|X_2| \leq \sqrt{2}\pi \tag{87a}$$

and

$$|X_3| \leq \frac{2\sqrt{2}}{\sqrt{3}}\pi \quad . \tag{87b}$$

Given X_2 and X_3, we must also consider

$$X_2' = X_2 + (\alpha_3 - \alpha_1)\sqrt{2}\pi \tag{88a}$$

$$X_3' = X_3 + (\alpha_1 - 2\alpha_2 + \alpha_3)\sqrt{(2/3)}\pi \tag{88b}$$

where

$$\alpha_i = -1,\ 0,\ \text{or}\ 1 \quad . \tag{89}$$

Now we wish to divide the X_2, X_3 space into regions corresponding to α choices which minimize R.

Consider first the special region, I, where

$$-\sqrt{2}\pi < X_2 < \sqrt{2}\pi \tag{90a}$$

$$-\frac{1}{\sqrt{6}}\pi < \frac{1}{\sqrt{6}}\pi \tag{90b}$$

$$R = X_3^2 \leq \frac{2}{3}\pi^2 \quad . \tag{91}$$

For this region, any increment of $\sqrt{2}\pi$ to X_2 or of $\sqrt{(2/3)}\pi$ to X_3 can never decrease R and hence when the data satisfies (90) no adjustment should be made.

Now we can cover the remainder of the data space (87) by translation of subregions of Region I and hence, conversely, every possible data point can be brought into Region I by the corresponding negative translation. The resulting decomposition of the data space is shown in Figure 22.

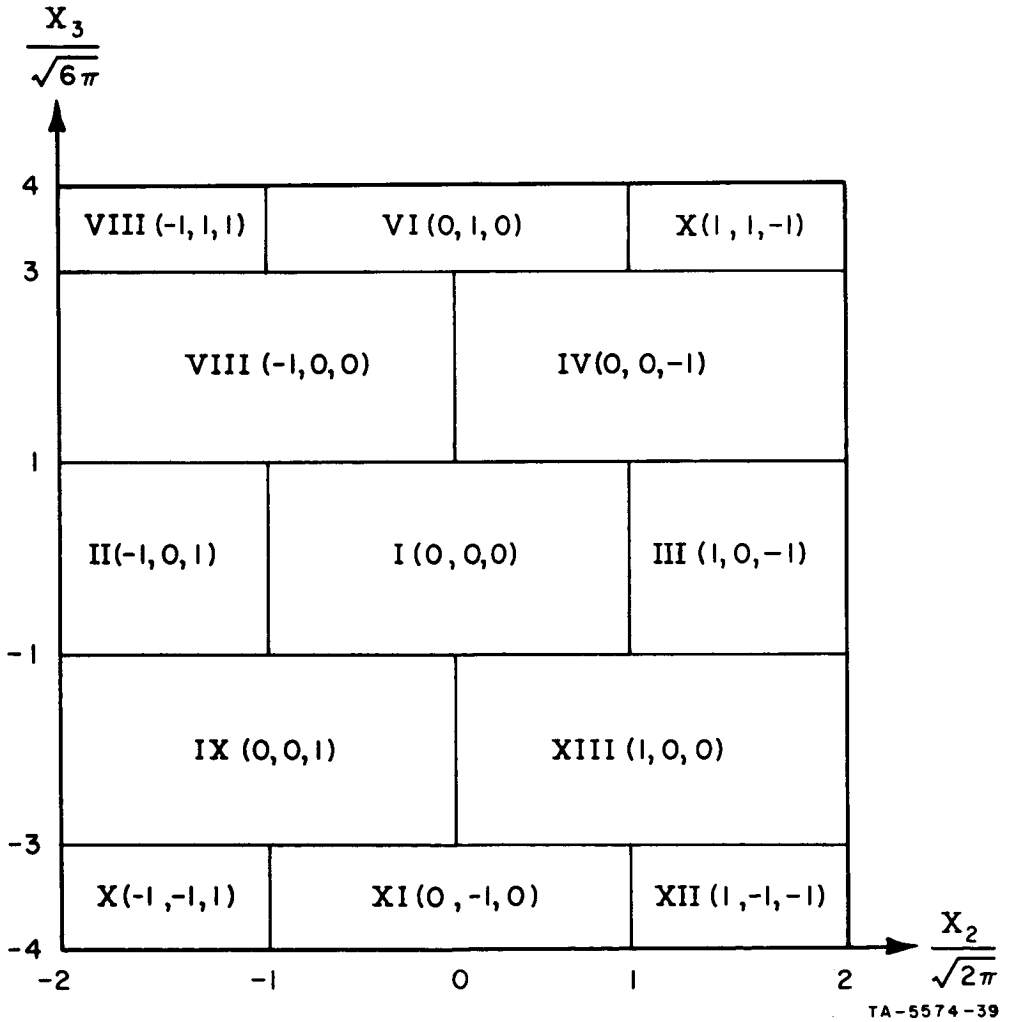

FIG. 22 REGIONS IN THE X_2–X_3 SPACE AND THE α-SET THAT CARRIES THEM INTO REGION I

III ANALYSIS

This section is designed to analyze the results obtained under the "work performed" section and to indicate avenues of future investigations.

A. ANTENNA CONFIGURATIONS

1. General Discussion

During the first half of the contract period, four specific antenna configurations have been considered for use as retrodirective antennas. Up to this time no serious consideration has been given to the effects of vehicle spin on the spectral quality with any of these configurations. On superficial consideration it appears that any configuration in which there is appreciable mutual coupling between the receiver elemental radiators will lead to a broadening of the spectrum received at each of these radiators. This would not only make the operation of phase-locked loops difficult but would, in general, degrade the quality of information being transmitted. Two configurations that obviously have such mutual coupling are the second and third types, which are discussed further below; both of these employ line-source radiators, and all of the amplifier/transmitters are active for all retrodirections. In the cylindrical-geodesic-lens configuration the mutual coupling is predominantly within the geodesic lens, while in the configuration using a circular array of omniazimuthal elements the coupling is obviously between the radiating elements.

In the case of the cylindrical-geodesic-lens biconical-horn antenna, previously analyzed,[1] spectral splitting is still present but, with the assumptions made, an incoming single frequency signal would be split into just two lines rather than a band of frequencies. It may well be possible to obviate the detrimental effects of this simple splitting by appropriate circuit design, whereas it presently appears unlikely that this can be done where there is strong interelement coupling.

In the fourth antenna configuration, that using discrete unidirectional line source radiators each with a switchable amplifier/transmitter, the detrimental effects of spectral splitting should be considerably easier to overcome. This configuration also appears to give an ERP as large as can be expected from any other configuration, in relation to the total number of elemental transmitters and radiators. For maximum ERP of the configuration considered the number of these elements active at any one time is only about one third the total number; if higher gain elemental radiators were used, this ratio of active elements would be even lower.

A more detailed analysis of each of the three configurations discussed in the body of this report is given below.

No attempt has yet been made, for any of the antenna configurations considered, to obtain an accurate prediction of gain, or ERP, that takes into account the effects of mutual coupling. This naturally varies for any two elements as a function of pointing angle. Even the approximate gain values computed so far are not entirely satisfactory, since the results are not always consistent when computed by different methods.

Although it has been shown[1] that a higher value of ERP will be obtained if the available RF power is distributed in an appropriate weighted manner between the radiators, rather than equally, all the computations discussed in this report assumed equal power distribution between the (active) elements. Equal power distribution was assumed because it is the only arrangement that is presently considered practical.

2. Cylindrical-Geodesic-Lens Discrete-Line-Source Antenna

The computed gain was found to be about 1 dB less than the postulated maximum possible value, and this can be considered acceptable. However the apparent amplitude modulation of ± 0.5 dB, as a function of vehicle spin, could prove quite unacceptable.

The effect of using different transmitter and receiver frequencies without some compensation is probably even more unacceptable but similar results would be obtained with almost any other configuration in which there is a few percent difference in the two frequencies.

It appears that the only significant parameter determining the ERP of a practical retrodirective antenna is the total number of transmitters,

and that other parameters such as the number of discrete line source radiators and the geometrical arrangements within the cylindrical lens are of relatively minor importance, with the general proviso—that the simpler, the better.

The possibility exists that, by using an odd number of elemental radiators, the modulation of ERP as a function of spin can be greatly reduced. No attempt has yet been made to investigate this.

3. Circular Array of Omnidirectional Elements

Calculations have been carried out for a circular array of omni-azimuthal elements, such as might be mounted at one end of a cylindrical space probe. The data presented are the pattern shape and directivity (gain) at the peak of the main beam for 30, 60, and 90 elements equally spaced around a 20-wavelength diameter circle. Although existing formulas were used in the calculations, the present work extends the numerical results to the case of large array diameters and large numbers of elements, which case is of interest in the application of retro-directive arrays to space probes. The shape of the radiation pattern was discussed in some detail as an aid in understanding why the directivity at the peak of the main beam is a function of the orientation of the array elements with respect to the main-beam direction.

So far, the directivity variation with array orientation has been calculated for only two numbers of elements in 20-wavelength diameter arrays. For 60 elements, the peak-to-peak variation of directivity was 0.25 dB; and for 61 elements, the variation was only 0.01 dB. These examples, plus the discussion given in the body of the report, indicate a preference for an odd number of elements. These figures apply for stationary arrays, but presumably there would be comparable directivity modulation as an array rotated on a spin-stabilized space probe. (These calculations did not take into account any effects that spectral splitting due to rotation might have on the phase-conjugate circuitry, or any phase errors introduced by differential Doppler shift across the array.) Also, these calculations neglect the effects on the array pattern of mutual coupling between array elements, as well as blocking of some elements by other elements. The performance of this somewhat idealized array can be used as a standard against which practical arrays can be compared.

The present calculations should be extended to include other numbers of elements so that the number of elements required in order to keep the directivity modulation below a given value can be established. Also, the analysis should be extended as much as practical to account for mutual coupling, blockage of some elements by others, and spinning of the array.

4. Switched-Element Retrodirective Array

The primary difference between the switched-element retrodirective array configuration and the three others that have been discussed is that switching logic is required on the vehicle in order to realize the maximum ERP. No attempt has yet been made to determine what added circuitry this switching would require, but the theoretical value of ERP when the appropriate switching is used appears to be very high. It should be noted that this large value of ERP, within a fraction of a dB of the postulated maximum value for any given total number of transmitting elements, is obtained even though only a fraction of these elements are used at any one time. It is, of course, necessary that each of the transmitters have higher output than would be necessary to obtain the same total radiated power if all the transmitting elements were active simultaneously. This higher value of "installed transmitter capacity", plus the switching circuitry, may be the price that has to be paid for a retrodirective antenna system that does not suffer from the spectral splitting effects of vehicle spin. This is because the antenna can be made with relatively low mutual coupling between the receiver/transmitter/radiator elements, leading in turn to a communication system in which the effects of spectral splitting of the retransmitted signal caused by spinning of the vehicle, is eliminated.

So far no attempt has been made to investigate the effects of vehicle spin on modulation of the ERP. In fact the number of radiating elements has only been assumed to be "large". Consideration of specific finite numbers of radiators is likely to indicate modulation of ERP with vehicle spin. The situation will be further complicated by the power switching operation which could also produce modulation.

B. ENVIRONMENTAL EFFECTS

Planetary reflection, such as from the moon and Venus, should be diffuse at retrodirective array frequencies greater than 1000 MHz. The

power reflectivity at the planet for diffuse reflection should not exceed 0.1. Variations in received power should not exceed 0.5 dB except when an array subaperture receives only a planetary signal, or in the unlikely event there is specular reflection from the planet. The power received at subapertures from planetary reflection will be no more than 10 percent below the power received from the direct signal (assuming a power reflectivity of 0.1).

The planetary reflected signal and the direct signal will, in general, be uncorrelated. A Doppler spread as large as hundreds of thousands of c/s can be expected in the planetary reflected signal.

The operation of a retrodirective array in planetary entry environment should be studied further. A comparison between a simple two-element retrodirective array and a single antenna on an entry capsule would be appropriate.

The effect of noise upon retrodirective array operation and upon the terminal receiving antenna operation should also be considered.

IV PROGRAM FOR NEXT QUARTER

Analysis of the several antenna configurations will continue, particularly the effect of vehicle spin on the received and retransmitted signal of a retrodirective antenna.

An attempt will be made to introduce the effect of mutual coupling into the analysis for the configuration that uses an array of isotropic radiators, and then to investigate the ramifications of this coupling on system operation.

Study will be continued of the systems aspects of the overall communication system, using some of the presently scheduled vehicles, such as the Voyager, as a basic concept to which adaptive antenna techniques might be applied.

The study of the concept of using adaptive antennas for direction finding will be continued.

Study of the environmental problems will be at a somewhat lower level than up to the present. The results will be reported in the Final Report rather than in the next (third) Quarterly Progress Report.

APPENDIX A

EXTENSION OF GODDARD SYSTEM TO EARTH/BUS/CAPSULE CONFIGURATION

PRECEDING PAGE BLANK NOT FILMED.

APPENDIX A

EXTENSION OF GODDARD SYSTEM TO EARTH/BUS/CAPSULE CONFIGURATION

This system is shown in Fig. A-1 and the corresponding spectra in Fig. A-2. We define the frequencies of the following signals as:

	Signal	Nominal Value (MHz)
f_{eB}	Carrier (w/mod) from earth to bus	2399
D_u	Doppler shift earth/bus path	
f_0	Bus local oscillator	30
f_{BC}	Carrier (w/mod) from bus to capsule	2491
D_C	Doppler shift bus/capsule path	
f_C	Capsule local oscillator	89
f_{CB1}	Carrier (w/mod) capsule to bus	2402
f_{CB2}	Carrier capsule to bus	2403
f_{Be}	Carrier bus to earth	1800
f_1	First subcarrier (w/mod)-bus to earth	1
f_2	Second subcarrier (w/mod)-bus to earth	2
f_3	Third subcarrier-bus to earth	3
D_0	$D_u/80$	

The signals received at the earth station have frequencies:

(1) $60\ f_0 + 3/4\ D_u$

(2) $60\ f_0 + 3/4\ D_u + 80\ f_0 - f_{eB} - D_u$

(3) $60\ f_0 + 3/4\ D_u + 83\ f_0 - f_{eB} - D_u + 2\ D_C - f_C$

$60\ f_0 + 3/4\ D_u + D_C - 80\ f_0 + 27\ f_C$

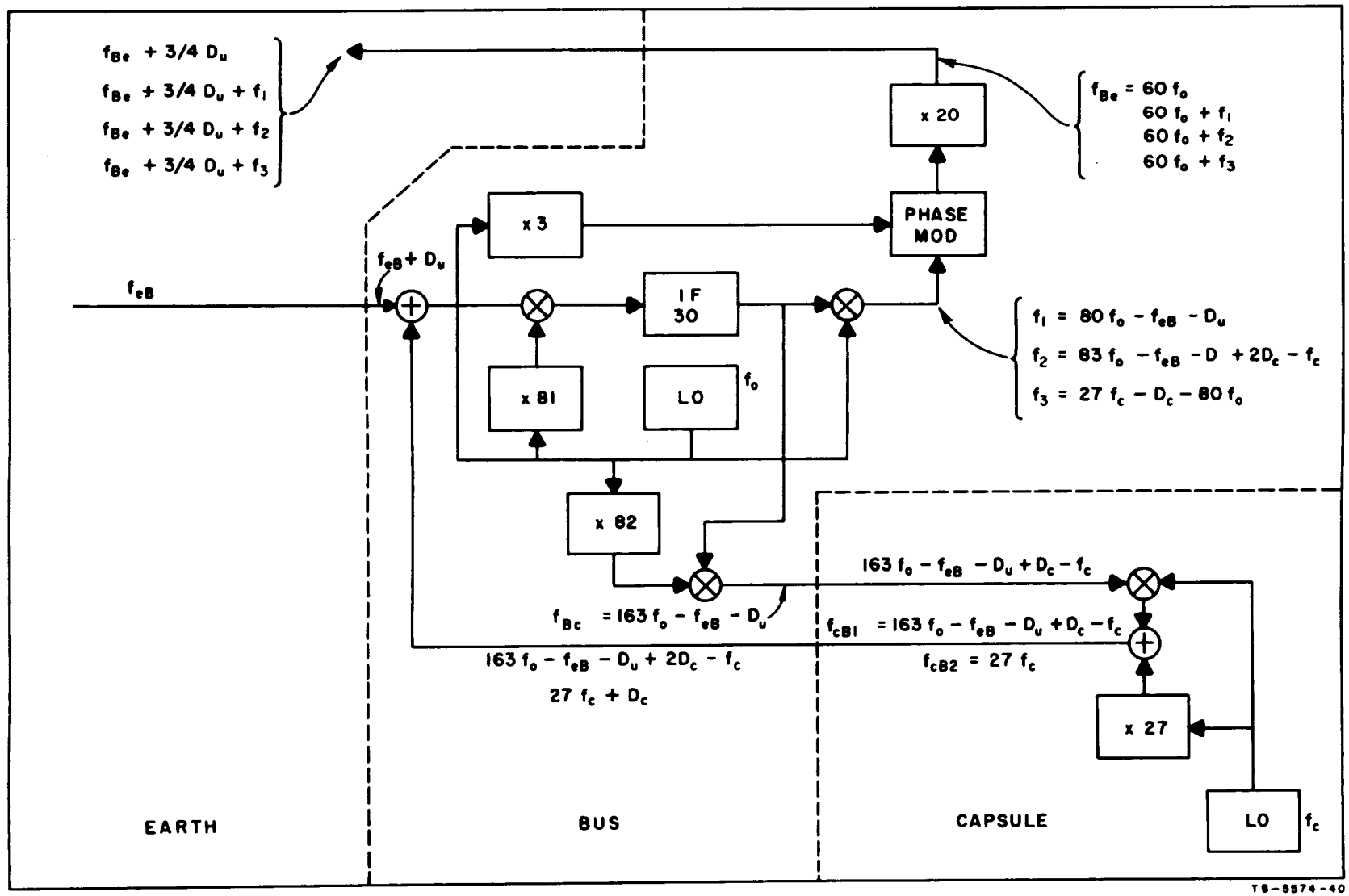

FIG. A-1 TWO-TRANSPONDER SYSTEM

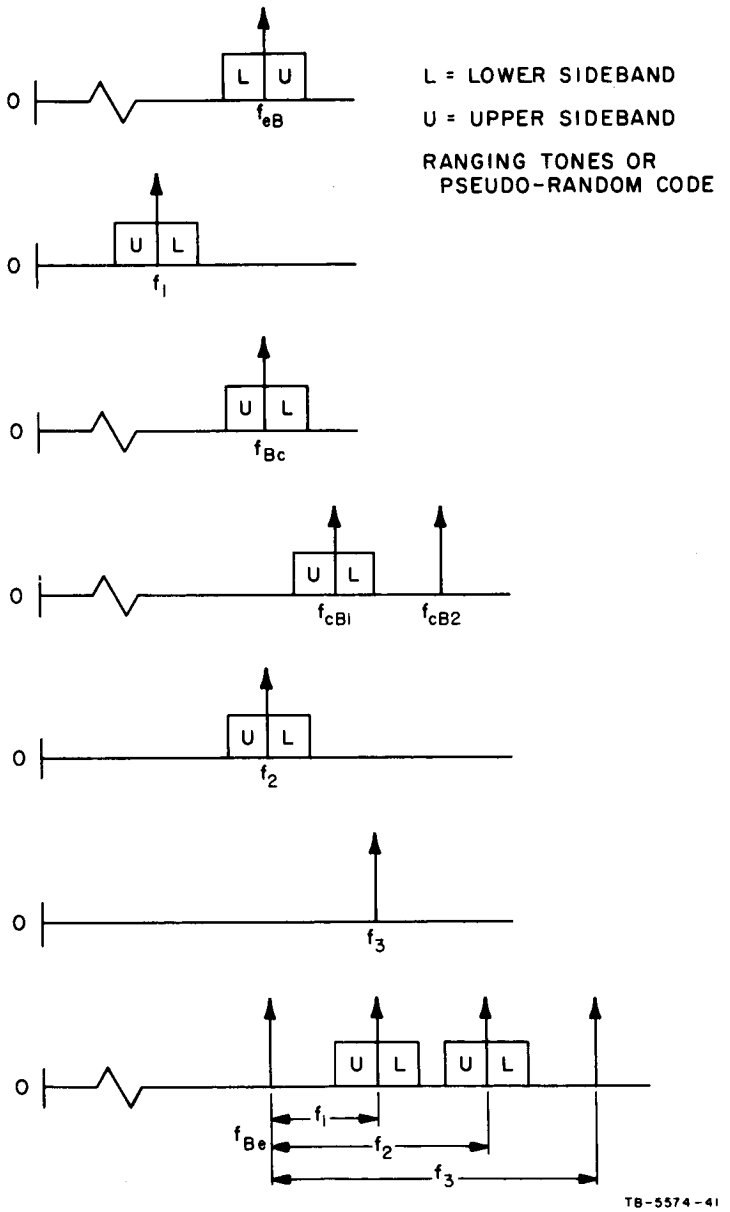

FIG. A-2 SPECTRA OF SIGNALS IN TWO-TRANSPONDER SYSTEM

Since f_{eB} is known at the receiver, signals (1) and (2) can be processed in a double phase-locked receiver to evaluate f_0 and D_u (see Fig. A-3). Then the remaining subcarriers C and d can be further processed to evaluate f_C and D_C (see Fig. A-4).

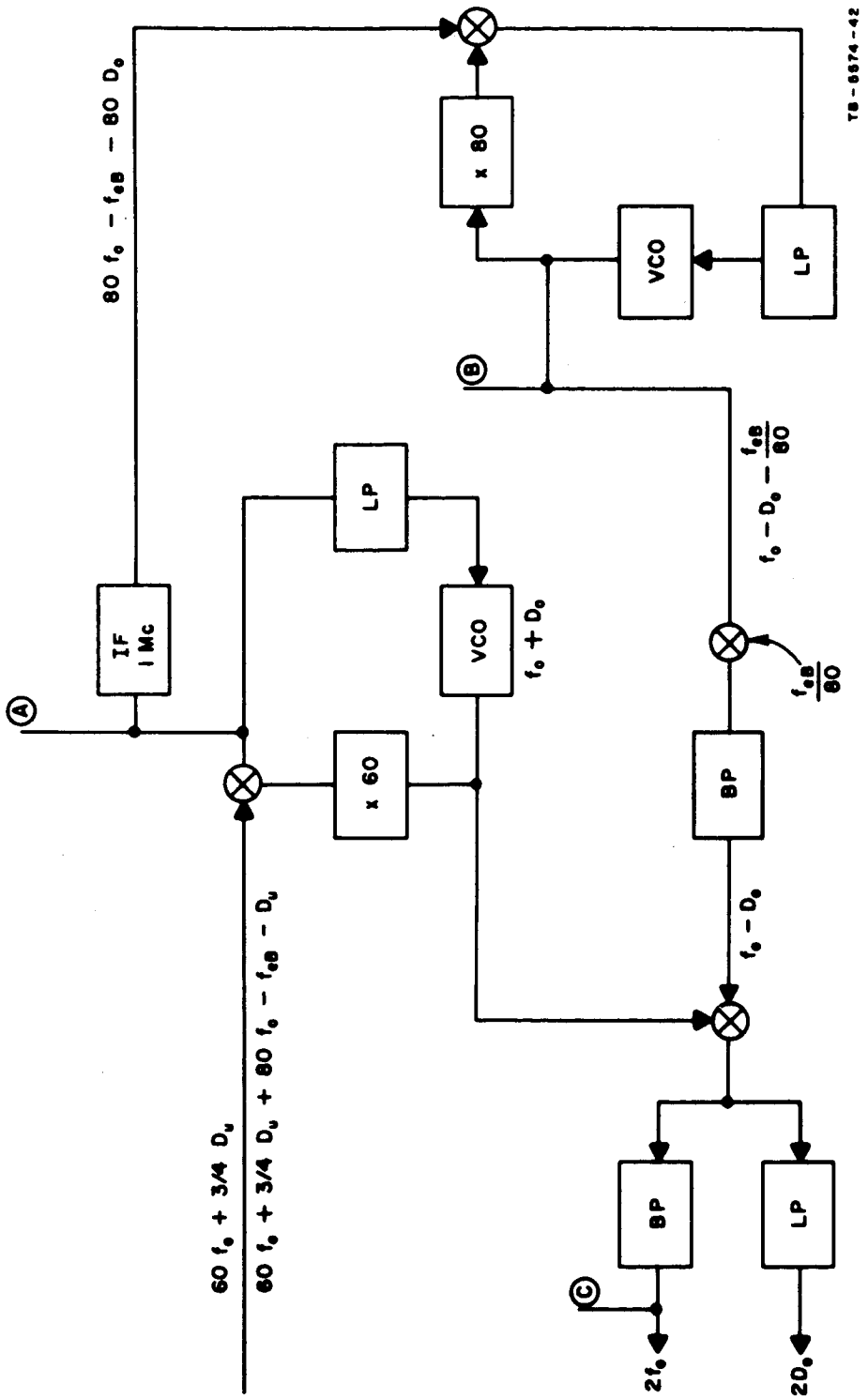

FIG. A-3 EVALUATION OF f_0 AND D_0

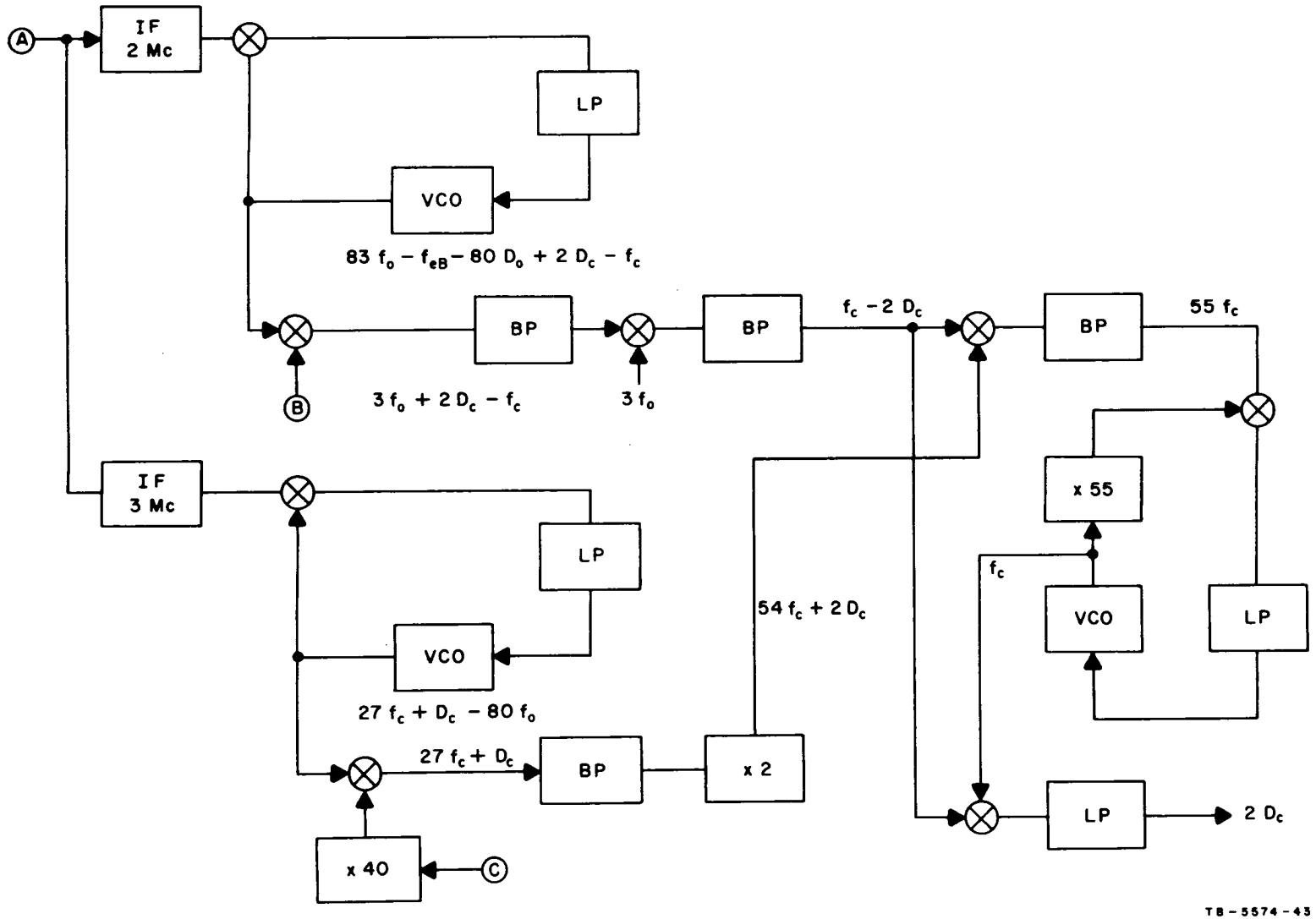

FIG. A-4 EVALUATION OF f_C AND D_C

APPENDIX B

CHANGE OF ORTHOGONAL BASES

APPENDIX B

CHANGE OF ORTHOGONAL BASES

Suppose we have an orthogonal basis in n-space and we have two non-colinear vectors in that space. We wish to rotate our basis so that in the new space the two axes define the plane containing the two given vectors and, of course, the remaining axes are perpendicular to that plane. We will require further that one of the new axes in the plane coincide with first of the given vectors. The set of axes perpendicular to the plane are, of course, not unique. However a particular set can be obtained as follows:

Define V_{1i} $i = 1, 2, \ldots n$ as the i-dimensional vector made up of the first i components of the first of the given two vectors.

Define V_{2i} $i = 1, 2, \ldots n$ as the i-dimensional vector made up of the first i components of

$$V_{2n} = V'_{2n} - (V_3^T \cdot \overline{V}_{1n})\overline{V}_{1n}$$

where V'_{2n} is the second given vector and $\overline{V}_{1n}$ is the unit vector in V_{1n} direction. If V_{1n} and V'_{2n} are already orthogonal, then $V_{2n} = V'_{2n}$.

Take V_{1n} and V_{2n} as the first two members of the new basis. The third vector can have 0's for $4, 5 \ldots n$ components and hence can be taken as the unique (within a multiplicative factor) vector orthogonal to V_{13} and V_{23}. Now we have (writing row vectors)

$$\left[\begin{array}{c|c} V_{13} & V_{1n} - V_{13} \\ V_{23} & V_{2n} - V_{23} \\ \hline V_{33} & 0 \end{array}\right]$$

To find a fourth vector, with 0's for its $5, 6, \ldots n$ components, consider V_{43} and its fourth component, V_4^i:

V_{33} is orthogonal to all linear combinations of V_{13} and V_{23} and hence if we take $V_{43} = \alpha V_{13} + \beta V_{23}$, V_{4n} will be orthogonal to V_{3n}. Since V_{44} must also be orthogonal to V_{1n} and V_{2n}, we have

$$V_{43} \cdot V_{13} + V_4^4 \cdot V_1^4 = 0$$

$$V_{43} \cdot V_{23} + V_4^4 \cdot V_2^4 = 0 \quad ,$$

or

$$(\alpha V_{13} + \beta V_{23}) \cdot V_{13} = -V_4^4 \cdot V_1^4$$

$$(\alpha V_{13} + \beta V_{23}) \cdot V_{23} = -V_4^4 \cdot V_2^4$$

or

$$(V_{13} \cdot V_{13})\alpha + (V_{23} \cdot V_{13})\beta = -V_4^4 \cdot V_1^4$$

$$(V_{23} \cdot V_{13})\alpha + (V_{23} \cdot V_{23})\beta = -V_4^4 \cdot V_2^4 \quad .$$

But these allow a unique solution for α and β in terms of V_4^4 which can be taken as 1 for convenience and, hence, V_{44} is uniquely determined. Now we have

$$\begin{bmatrix} V_{13}|V_1^4| & V_{1n} - V_{14} \\ V_{23}|V_2^4| & V_{2n} - V_{24} \\ V_{33}| & 0 \\ V_{43}|1| & 0 \end{bmatrix}$$

Suppose we have continued in similar fashion to obtain j vectors, then we take the $j + 1st$ vector as follows

$$V_{j+1,n}(\alpha V_{1j} + \beta V_{2j}),\ 1,\ 0 \ldots . 0 \quad .$$

Since no vector in the set of 3 to j has no nonzero component with index greater than j and is orthogonal to all linear combinations of V_{1n} and V_{2n}, $V_{j+1,n}$ is orthogonal to all such vectors. The proper α and β to make $V_{j+1,n}$ orthogonal to V_{1n} and V_{2n} are the unique solution of

$$(V_{1j} \cdot V_{1j})\alpha + (V_{1j} \cdot V_{2j})\beta = -V_1^{j+1}$$

$$(V_{1j} \cdot V_{2j})\alpha + (V_{2j} \cdot V_{2j})\beta = -V_2^{j+1}$$

Consider, as an example, sixth-dimensional space with

$$V_1 = 1 \quad 1 \quad 1 \quad 1 \quad 1 \quad 1$$

$$V_2 = -5 \quad -3 \quad -1 \quad 1 \quad 3 \quad 5$$

$V_{12} \cdot V_{12} = 2$ $\qquad$ $V_{12} \cdot V_{22} = -8$

$V_{22} \cdot V_{22} = 34$ $\qquad$ $V_1^3 = 1$ $\qquad$ $V_2^3 = -1$

$2\alpha = 8\beta = -1$ $\qquad$ $\alpha = 6\frac{1}{2}$

$V_3^3 = 1$

$-8\alpha + 34\beta = 1$ $\qquad$ $\beta = 1\frac{1}{2}$

or

$$\alpha' = -13 \quad \beta' = -3 \quad V_3^{3\prime} = 2$$

$$V_3 = 2 \quad -4 \quad 2 \quad 0 \quad 0 \quad 0$$

$V_{13} \cdot V_{13} = 3$ $\qquad$ $V_{13} \cdot V_{23} = -9$

$V_{23} \cdot V_{23} = 35$ $\qquad$ $V_1^4 = 1$ $\qquad$ $V_2^4 = 1$

$3\alpha - 9\beta = -1$ $\qquad$ $\alpha = -\frac{11}{6}$

$V_4^4 = 1$

$-9\alpha + 35\beta = -1$ $\qquad$ $\beta = -\frac{1}{2}$

or

$$\alpha' = -11 \quad \beta'' = -3 \quad V_4^{4\prime} = 6$$

$$V_4 = 4, -2, -8, 6, 0, 0$$

$$V_{14} \cdot V_{14} = 4 \qquad V_{14} \cdot V_{24} = -8$$

$$V_{24} \cdot V_{24} = 36 \qquad V_1^5 = 1 \qquad V_2^5 = 3$$

$$4\alpha - 8\beta = -1 \qquad \alpha = -\frac{3}{4}$$

$$V_5^5 = 1$$

$$-8\alpha + 36\beta = -3 \qquad \beta = -\frac{1}{4}$$

or

$$\alpha' = -3 \qquad \beta' = -1 \qquad V_5^{5\prime} = 4$$

$$V_5 = 2\ 0\ -2\ -4\ 4\ 0$$

$$V_{15} \cdot V_{15} = 5 \qquad V_{15} \cdot V_{25} = -5$$

$$V_{25} \cdot V_{25} = 45 \qquad V_1^6 = 1 \qquad V_2^6 = 5$$

$$5\alpha - 5\beta = 1 \qquad \alpha = \frac{7}{20}$$

$$V_6^6 = 1$$

$$-5\alpha + 45\beta = 5 \qquad \beta = \frac{3}{20}$$

or

$$\alpha' = 7 \qquad \beta' = 3 \qquad V_6^{6\prime} = 20$$

$$V_6 = -8\ -2\ 4\ 10\ 16\ 20$$

In summary (after reduction and making leading terms positive)

$$V_1 = 1\ 1\ 1\ 1\ 1\ 1$$
$$V_2 = 5\ 3\ 1\ -1\ -3\ -5$$
$$V_3 = 1\ -2\ 1\ 0\ 0\ 0$$
$$V_4 = 2\ -1\ -4\ 3\ 0\ 0$$
$$V_5 = 1\ 0\ -1\ -2\ 2\ 0$$
$$V_6 = 4\ 1\ -2\ -5\ -8\ -10$$

REFERENCES

1. C. A. Hacking and J. A Martin "Study and Application of Retrodirective and Self-Adaptive Electromagnetic Wave Controls to a Mars Probe," First Quarterly Report, Contract NAS 2-2933, SRI Project 5574, Stanford Research Institute, Menlo Park, California (November 1965).

2. E. M. Butz-Philipp, "Spherical Retrodirective Array," *IEEE Trans.* AP-12, No. 2, pp. 187-194 (March 1964).

3. C. C. Cutler, R. Kompfner, and L. C. Tillotson, "A Self Steering Array Repeater," *Bell System Tech. J.* **43**, No. 5, pp. 2013-2032 (September 1963).

4. H. L. Knudsen, "The Necessary Number of Elements in a Direction Ring Aerial," *J. Appl. Phys.* **22**, No. 11, pp. 1299-1306 (November 1951).

5. H. Stenzel, *Elek. Nachr.-Tech.* **6**. pp. 165-181 (May 1929).

6. C. E. Hickman, H. P. Neff, and J. D. Tillman, "The Theory of Single-Ring Circular Antenna Arrays," Scientific Report 4, AFCRL 543, Contract AF 19(604)-4967, University of Tennessee College of Engineering, Knoxville, Tennessee (1 July 1961), AD 262 662.

7. W. T. Patton and J. D. Tillman, "An Analysis of the Terminal Properties of a Circular Antenna Array with a Synthesis Technique for Obtaining a Prescribed Radiation Pattern," Scientific Report 2, AFCRC-TN-58-148, Contract AF 19(604)-1657, University of Tennessee College of Engineering, Knoxville, Tennessee (1 June 1958). AD 152 379.

8. H. A. Rosen, "Directive Array for a Spinning Vehicle," *Proc. 1962 National Telemetering Conference,* **1**, Sec. 1-4 (23-25 May 1962).

9. E. Jahnke and F. Emde, *Tables of Functions with Formulae and Curves,* Fourth Ed., Chapter 8, (Dover Publications, Inc., New York, New York, 1945).

10. G. N. Watson, *A Treatise on the Theory of Bessel Functions,* Second Ed., Chapter 8, (Macmillan Company, New York, New York, 1948).

11. W. W. Hansen and J. R. Woodyard, "A New Principle in Directional Antenna Design," *Proc. IRE,* **26**, No. 3, pp. 333-345 (March 1938).

12. H. Page, "Radiation Resistance of Ring Aerials," *Wireless Engineer,* **25**, pp. 102-109 (April 1948).

13. H. Page, "Ring Aerial Systems," *Wireless Engineer,* **25**, pp. 308-315 (October 1948).

14. J. D. Tillman, W. T. Patton, C. E. Blakely, and F. V. Schultz, "The Use of a Ring Array as a Skip Range Antenna," *Proc. IRE,* **43**, No. 11, pp. 1655-1660 (November 1955).

15. V. A. Hughes, "Roughness of the Moon as a Radar Reflector," *Nature* **186**, No. 4728, pp. 873-874 (1960).

16. R. L. Leadabrand, R. B. Dyce, A. Frediksen, R. I. Presnell, and J. C. Schlobohm, "Radio Frequency Scattering from the Surface of the Moon," *Proc. IRE,* **48**, pp. 932-933 (May 1960).

17. R. B. Dyce and R. A. Hill, Lunar Echoes Received on Spaced Receivers at 106.1 Mc," *Proc. IRE* **48**, pp. 934-935 (May 1960).

18. M. I. Skolnik, *Introduction to Radar Systems,* Chapter 14, (McGraw-Hill Book Company, Inc., New York, 1962).

19. P. Beckmann and A. Spizzichino, *The Scattering of Electromagnetic Waves From Rough Surfaces.* pp. 334-340 (The MacMillan Company, New York, 1963).

20. G. C. Kronmiller, Jr. and E. J. Baghdady "The Goddard Range and Range-Rate Tracking System: Concept, Design, and Performance," Report X-531-65-403 Goddard Space Flight Center, Greenbelt, Maryland (October 1965).

UNCLASSIFIED

Security Classification

DOCUMENT CONTROL DATA - R&D

(Security classification of title, body of abstract and indexing annotation must be entered when the overall report is classified)

1. ORIGINATING ACTIVITY (Corporate author)	2a. REPORT SECURITY CLASSIFICATION
Stanford Research Institute Menlo Park, California 94025	UNCLASSIFIED
	2b. GROUP

3. REPORT TITLE

STUDY AND APPLICATIONS OF RETRODIRECTIVE AND SELF-ADAPTIVE ELECTROMAGNETIC WAVE CONTROLS TO A MARS PROBE

4. DESCRIPTIVE NOTES *(Type of report and inclusive dates)*

1 Oct. to 31 Dec. 1965

5. AUTHOR(S) *(Last name, first name, initial)*

Hacking, Colin A. Dawson, Charles H. Kunzelman, Richard C.
Martin, James A. Robinson, Lloyd A.

6. REPORT DATE	7a. TOTAL NO. OF PAGES	7b. NO. OF REFS
February 1966	110	20

8a. CONTRACT OR GRANT NO.	9a. ORIGINATOR'S REPORT NUMBER(S)
NAS 2-2933	
b. PROJECT NO.	Second Quarterly Report, SRI Project 5574
c.	9b. OTHER REPORT NO(S) *(Any other numbers that may be assigned this report)*
d.	

10. AVAILABILITY/LIMITATION NOTICES

11. SUPPLEMENTARY NOTES	12. SPONSORING MILITARY ACTIVITY
	National Aeronautics and Space Administration Technical Information Division Ames Research Center Moffett Field, California

13. ABSTRACT

Computer studies have been continued of three different cylindrical antenna configurations that could be used as adaptive arrays for deep space vehicles. Analysis of the effects of vehicle spin on gain modulation has been made. Some effects of spin on spectral splitting are superficially discussed but have not yet been analyzed.

The effects of planetary reflections on a retrodirective array system have been studied.

Some system aspects of a planetary mission employing retrodirective arrays are considered. A start has also been made on studying the use of an adaptive array to provide navigational information such as angle of arrival of a signal.

DD FORM 1 JAN 64 1473

UNCLASSIFIED

Security Classification

14. KEY WORDS	LINK A		LINK B		LINK C	
	ROLE	WT	ROLE	WT	ROLE	WT

INSTRUCTIONS

1. ORIGINATING ACTIVITY: Enter the name and address of the contractor, subcontractor, grantee, Department of Defense activity or other organization *(corporate author)* issuing the report.

2a. REPORT SECURITY CLASSIFICATION: Enter the overall security classification of the report. Indicate whether "Restricted Data" is included. Marking is to be in accordance with appropriate security regulations.

2b. GROUP: Automatic downgrading is specified in DoD Directive 5200.10 and Armed Forces Industrial Manual. Enter the group number. Also, when applicable, show that optional markings have been used for Group 3 and Group 4 as authorized.

3. REPORT TITLE: Enter the complete report title in all capital letters. Titles in all cases should be unclassified. If a meaningful title cannot be selected without classification, show title classification in all capitals in parenthesis immediately following the title.

4. DESCRIPTIVE NOTES: If appropriate, enter the type of report, e.g., interim, progress, summary, annual, or final. Give the inclusive dates when a specific reporting period is covered.

5. AUTHOR(S): Enter the name(s) of author(s) as shown on or in the report. Enter last name, first name, middle initial. If military, show rank and branch of service. The name of the principal author is an absolute minimum requirement.

6. REPORT DATE: Enter the date of the report as day, month, year; or month, year. If more than one date appears on the report, use date of publication.

7a. TOTAL NUMBER OF PAGES: The total page count should follow normal pagination procedures, i.e., enter the number of pages containing information.

7b. NUMBER OF REFERENCES: Enter the total number of references cited in the report.

8a. CONTRACT OR GRANT NUMBER: If appropriate, enter the applicable number of the contract or grant under which the report was written.

8b, 8c, & 8d. PROJECT NUMBER: Enter the appropriate military department identification, such as project number, subproject number, system numbers, task number, etc.

9a. ORIGINATOR'S REPORT NUMBER(S): Enter the official report number by which the document will be identified and controlled by the originating activity. This number must be unique to this report.

9b. OTHER REPORT NUMBER(S): If the report has been assigned any other report numbers *(either by the originator or by the sponsor)*, also enter this number(s).

10. AVAILABILITY/LIMITATION NOTICES: Enter any limitations on further dissemination of the report, other than those imposed by security classification, using standard statements such as:

(1) "Qualified requesters may obtain copies of this report from DDC."

(2) "Foreign announcement and dissemination of this report by DDC is not authorized."

(3) "U. S. Government agencies may obtain copies of this report directly from DDC. Other qualified DDC users shall request through _____."

(4) "U. S. military agencies may obtain copies of this report directly from DDC. Other qualified users shall request through _____."

(5) "All distribution of this report is controlled. Qualified DDC users shall request through _____."

If the report has been furnished to the Office of Technical Services, Department of Commerce, for sale to the public, indicate this fact and enter the price, if known.

11. SUPPLEMENTARY NOTES: Use for additional explanatory notes.

12. SPONSORING MILITARY ACTIVITY: Enter the name of the departmental project office or laboratory sponsoring *(paying for)* the research and development. Include address.

13. ABSTRACT: Enter an abstract giving a brief and factual summary of the document indicative of the report, even though it may also appear elsewhere in the body of the technical report. If additional space is required, a continuation sheet shall be attached.

It is highly desirable that the abstract of classified reports be unclassified. Each paragraph of the abstract shall end with an indication of the military security classification of the information in the paragraph, represented as *(TS)*, *(S)*, *(C)*, or *(U)*.

There is no limitation on the length of the abstract. However, the suggested length is from 150 to 225 words.

14. KEY WORDS: Key words are technically meaningful terms or short phrases that characterize a report and may be used as index entries for cataloging the report. Key words must be selected so that no security classification is required. Identifiers, such as equipment model designation, trade name, military project code name, geographic location, may be used as key words but will be followed by an indication of technical context. The assignment of links, roles, and weights is optional.